

A robust approach for ROC curves with covariates

Ana M. Bianco¹, Graciela Boente¹ and Wenceslao González–Manteiga²

¹ Universidad de Buenos Aires and CONICET

² Universidad de Santiago de Compostela

Abstract

The Receiver Operating Characteristic (ROC) curve is a useful tool that measures the discriminating power of a continuous variable or the accuracy of a pharmaceutical or medical test to distinguish between two conditions or classes. In certain situations, the practitioner may be able to measure some covariates related to the diagnostic variable which can increase the discriminating power of the ROC curve. To protect against the existence of atypical data among the observations, a procedure to obtain robust estimators for the ROC curve in presence of covariates is introduced. The considered proposal focusses on a semiparametric approach which fits a location-scale regression model to the diagnostic variable and considers empirical estimators of the regression residuals distributions. Robust parametric estimators are combined with adaptive weighted empirical distribution estimators to down-weight the influence of outliers. The uniform consistency of the proposal is derived under mild assumptions. A Monte Carlo study is carried out to compare the performance of the robust proposed estimators with the classical ones both, in clean and contaminated samples. A real data set is also analysed.

AMS Subject Classification: 62F35

Key words and phrases: Covariates; Robustness, ROC curves; Parametric regression

1 Introduction

The Receiver Operating Characteristic (ROC) curve is a useful tool to size up the capability of a continuous variable or the accuracy of a pharmaceutical or medical test to distinguish between two conditions. ROC curves are a very well known technique in medical studies where a continuous variable or marker (biomarker) is used to diagnose a disease or to evaluate the progression of a disease. The use of ROC curves has become more and more popular in medicine from the early 60's (see Goncalves *et al.*, 2014, for a historical note and Krzanowsk and Hand, 2009 for further details).

ROC curves can also be extended to other general statistical situations such as classification or discrimination, where we typically have a set of individuals or items assigned to one of two classes on the basis of disposable information of that individual. A ROC curve is essentially a plot that represents the diagnostic skill of a binary classifier as the discriminating threshold varies. Assignations are not perfect and may lead to classification errors. In fact, during the assignment procedure some errors may occur, in the sense that an individual or object may be allocated into a wrong class. At this point, ROC curves become an interesting strategy either to evaluate the quality of a given assignment rule or to compare two available procedures.

To be more precise, assume that we deal with two populations, henceforth, identified as diseased (D) and healthy (H) and that a continuous score usually called *biomarker* or *diagnostic variable*, Y , is considered for the assignment purpose and whose rule is based on a cut-off value c . Thus, according to this assignment rule, an individual is classified as diseased if $Y \geq c$ and as healthy when $Y < c$. Let F_D be the distribution of the marker on the diseased population and F_H the distribution of Y in the healthy one. From now on, for practical reasons, we denote as $Y_D \sim F_D$ the marker in the diseased population and $Y_H \sim F_H$ the score in the healthy one. Without loss of generality, we will assume that Y_D is stochastically greater than Y_H , that is, $\mathbb{P}(Y_D \leq c) \leq \mathbb{P}(Y_H \leq c)$ for all c . It

is clear that the classification errors depend on the threshold c . Therefore, it becomes of interest to study the triplets $\{(c, 1 - F_H(c), 1 - F_D(c)), c \in \mathbb{R}\}$, which describes a geometrical object called ROC curve, that reflects the discriminatory capability of the marker. This suggests a different parametrization of this curve in terms of the false positive rate, $1 - F_H(c)$, leading to $\{(p, 1 - F_D(F_H^{-1}(1 - p))), p \in (0, 1)\}$ and therefore, to $\text{ROC}(p) = 1 - F_D(F_H^{-1}(1 - p))$, $p \in (0, 1)$. In this manner, the ROC curve is a complete picture of the performance of the assignment procedure over all the possible threshold values.

In practical situations, the discriminatory effectiveness of the biomarker may be improved by several factors. Thus, when for each individual there is additional information contained in measured covariates, it is sensible to include them in the ROC analysis. Through examples Pepe (2003) illustrates how the discriminatory capability of a test is improved by the presence of covariates. For an overview on this topic, we refer to Pardo-Fernández *et al.* (2014). In brief, we may say that the information registered all along the covariates may impact the discrimination capability of the ROC curve. In this situation, in order to have a deeper comprehension of the effect of the covariates, it would be advisable to incorporate this additional covariates information to the ROC analysis instead of considering a *joint* ROC curve, that may lead to oversimplification. This issue can be accomplished in different ways. In the direct methodology, the ROC curve is directly regressed onto the covariates by means of a generalized linear model. Among others, Alonzo and Pepe (2002), Pepe (2003) and Cai (2004) follow this approach. In contrast, in the induced methodology, the markers distribution in each population is modelled separately in terms of the covariates and just after, the induced ROC curve is computed. The papers by Pepe (1998), Faraggi (2003), González-Manteiga *et al.* (2011) and Rodríguez-Álvarez *et al.* (2011a) go in this direction. Besides, Inácio de Carvalho *et al.* (2013) follow a Bayesian nonparametric approach to fit covariate-dependent ROC curves using probability models in each population, while Rodríguez-Álvarez *et al.* (2011b) perform a

comparative study of the direct and induced methodologies. In such case, if we denote as \mathbf{X}_D and \mathbf{X}_H the covariates for the disease and healthy populations, the conditional ROC curve is defined as

$$\text{ROC}_{\mathbf{x}}(p) = 1 - F_D(F_H^{-1}(1 - p|\mathbf{x})|\mathbf{x}), \quad (1)$$

where $F_j(\cdot|\mathbf{x})$ stands for conditional distribution of $Y_j|\mathbf{X}_j = \mathbf{x}$, $j = H, D$. In this paper, we focus on the latter approach through a general regression model.

The general methodology to estimate the conditional ROC curve consists in a plug-in procedure where estimators of the regression and of the variance functions together with empirical distribution and quantile function estimators based on the residuals are plugged into the general expression of the conditional ROC curve. Pepe (1997, 1998, 2003), Faraggi (2003), González-Manteiga *et al.* (2011) propose estimators that implement these ideas. Since most of these estimators are based on classical least squares procedures or local averages, they may be very sensitive to anomalous data or small deviations from the model assumptions. The bi-normal model, in which both populations are assumed to be normal, is a very popular choice to fit a ROC curve and one justification for its broad use is its robustness. The term robustness may have different interpretations; in fact, Gonçalves *et al.* (2014) discuss the scope of the so-called robustness in the ROC curve scenario. Walsh (1997) performs a simulation study that shows that the bi-normal estimator is sensitive to model misspecifications and to the location of the decision thresholds.

In this paper, we focus on robustness, that is, resistance to deviations from the underlying model plus efficiency when this central model holds. During the last decades, robust statistics has pursued the aim of developing procedures that enable reliable inference results, even if small deviations from the model assumptions occur or in the presence of a moderate percentage of outliers. Even when these efforts have been sustained over time across different statistical areas, up to our knowledge, ROC curves have received little attention from this robustness point of view. When no covariates are available, robust estimators of the area under the ROC curve were given in Greco and Ventura (2011)

assuming that the distribution functions are known up to a finite-dimensional parameter (see also Farcomeni and Ventura, 2012). In this sense, when covariates are recorded to improve the discrimination power of the biomarker, the main contribution of our paper is to bridge the gap between ROC curves and robustness. We achieve this goal by fitting a location-scale regression model to the diagnostic variable and considering adaptive empirical estimators of the regression residuals distributions. In this respect, our proposal is semiparametric since the errors distribution is not assumed to be known, for example, as in the bi-normal model.

Our motivating example consists of the real dataset of a marker for diabetes previously analysed in Faraggi (2003) and Pardo-Fernández *et al.* (2014), in which we add to their analysis a robust perspective focussing on the potential effect of influential data. The observations, that come from a population-based pilot survey of diabetes mellitus in Cairo, Egypt, consist of postprandial blood glucose measurements (Y) from a fingerstick in 286 subjects who were divided into healthy (198) and diseased (88) groups according to gold standard criteria of the World Health Organization (1985). It is believed that the aging process may be associated with resistance or relative insulin deficiency among healthy people, therefore postprandial fingerstick glucose levels would be expected to be higher for older persons who do not have diabetes. According to this belief, Smith and Thompson (1996) adjust the ROC curve analysis for covariate information using age (X). The obtained ROC curve of the transformed biomarker is given in Figure 1 together with the ROC curve obtained after removing the 6 outliers detected in the healthy sample through a robust regression fit. Figure 1 also displays the ROC curve built using the naive approach of using robust regression estimators combined with the usual empirical distribution and quantile function estimators based on the residuals. These plots illustrate that the use of robust regression and variance estimators are not enough to protect the estimation of the ROC curve from the influence of atypical data. This effect may be explained by the fact that large residuals are still present when empirical distribution estimators are computed.

This motivates the need of defining appropriate robust estimators of the ROC curve.

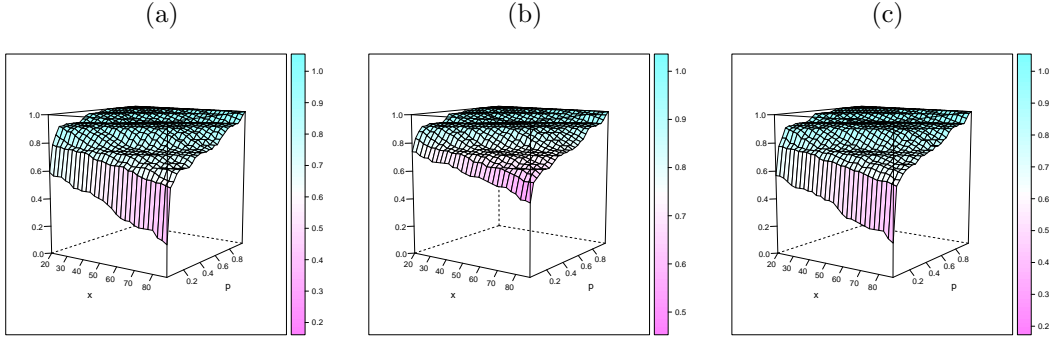


Figure 1: Estimated ROC surfaces for the Diabetes Data using Age (X) as covariate: (a) Classical estimator, (b) Classical estimator without the detected outliers and (c) Naive estimator.

In the rest of the paper we will introduce a robust proposal and we will study some of its properties. The paper is organized as follows. Section 2 reviews some general concepts regarding the conditional ROC curve, while Section 3 introduces the robust proposal to estimate the ROC curve focussing in the special situation of a parametric regression model. Section 4 presents some consistency results of the proposed procedure. Finally, in Section 5, a numerical study is conducted to examine the small sample properties of the proposed procedures under a linear and a nonlinear regression model, while the advantages of the proposed methodology are illustrated in Section 6 on a real data set. All proofs are relegated to the Appendices.

2 Preliminaries

In this section, we recall the approach considered to model the induced ROC curve when covariates are measured. For that purpose, denote as Y_D and \mathbf{X}_D the biomarker and the covariates measured in the diseased population and as Y_H and \mathbf{X}_H the corresponding ones in the healthy individuals. For the sake of simplicity, we will assume that the covariates of interest are the same in both populations.

A general way to include covariates is through a general location–scale regression model which, for simplicity of presentation, we assume homoscedastic, that is,

$$Y_D = \mu_{0,D}(\mathbf{X}_D) + \sigma_{0,D} \epsilon_D , \quad (2)$$

$$Y_H = \mu_{0,H}(\mathbf{X}_H) + \sigma_{0,H} \epsilon_H , \quad (3)$$

where, for $j = D, H$, $\mu_{0,j}$ is the true regression function and $\sigma_{0,j}$ corresponds to the model dispersion, respectively. It is also assumed that the errors $\epsilon_j \sim G_j$ are independent of \mathbf{X}_j , for $j = D, H$ and have scale 1 to properly identify $\sigma_{0,j}$. Furthermore, to identify the regression function avoiding moment conditions, we will assume that G_j has a symmetric distribution. Denote as \mathcal{S} the common support of \mathbf{X}_D and \mathbf{X}_H . It is worth noticing that since the errors and the covariates are independent, for a given $\mathbf{x} \in \mathcal{S}$, we have that

$$\begin{aligned} F_{Y_D}(y|\mathbf{x}) &= F_{Y_D|X_D}(y|\mathbf{x}) = \mathbb{P}(Y_D \leq y | \mathbf{X}_D = \mathbf{x}) = \mathbb{P}(\mu_{0,D}(\mathbf{X}_D) + \sigma_{0,D} \epsilon_D \leq y | \mathbf{X}_D = \mathbf{x}) \\ &= G_D \left(\frac{y - \mu_{0,D}(\mathbf{x})}{\sigma_{0,D}} \right) . \end{aligned}$$

Analogously, we get that the conditional distribution in the healthy distribution satisfies

$$F_{Y_H}(y|\mathbf{x}) = F_{Y_H|X_H}(y|\mathbf{x}) = G_H \left(\frac{y - \mu_{0,H}(\mathbf{x})}{\sigma_{0,H}} \right) .$$

As a consequence, the quantiles of the conditional distributions are related to those of the errors through $F_j^{-1}(p|\mathbf{x}) = \sigma_{0,j} G_j^{-1}(p) + \mu_{0,j}(\mathbf{x})$, for $j = D, H$, where $G_j^{-1}(\cdot)$ denotes the quantile function of the errors ϵ_j . Thus, the conditional ROC curve given $\mathbf{x} \in \mathcal{S}$ defined in (1) can be computed as

$$\text{ROC}_{\mathbf{x}}(p) = 1 - G_D \left(\frac{\mu_{0,H}(\mathbf{x}) - \mu_{0,D}(\mathbf{x})}{\sigma_{0,D}} + \frac{\sigma_{0,H}}{\sigma_{0,D}} G_H^{-1}(1 - p) \right) . \quad (4)$$

One advantage of this approach is that it enables a very general modelling of the regression functions $\mu_{0,j}$, for $j = D, H$, since this task can be accomplished from different perspectives. This means that according to the information about the relationship between the biomarker and the covariates and the user's preferences, the regression functions may be

modelled parametrically or either nonparametrically or partly parametrically, even when these last two approaches will be subject of future work.

As mentioned in the Introduction, expression (4) of the conditional ROC curve suggests a natural estimation procedure. First, compute estimators of the regression function and the dispersion parameter which allow to obtain the corresponding residuals. Then, estimate G_D and G_H^{-1} by empirical distribution and quantile function estimators based on the residuals, respectively. Finally, using these estimators in (4) and plugging there-in the obtained estimators of the regression functions and variance parameters, we obtain an estimator of the conditional ROC. Our goal is to introduce a procedure to get reliable and stable $\text{ROC}_{\mathbf{x}}$ estimators, even when a moderate percentage of outliers arise in one sample or in both of them.

Different summary measures of the ROC curve are useful to sum up particular features of the curve. One of the most popular indices is the conditional *area under the curve* ($\text{AUC}_{\mathbf{x}}$), which is computed as $\text{AUC}_{\mathbf{x}} = \int_0^1 \text{ROC}_{\mathbf{x}}(p)dp$.

3 Proposal

3.1 The general procedure

Suppose that we have a sample from the diseased population, $(y_{D,i}, \mathbf{x}_{D,i})$, $1 \leq i \leq n_D$, that verifies model (2) and one from the healthy population, $(y_{H,i}, \mathbf{x}_{H,i})$, $1 \leq i \leq n_H$, verifying model (3). Furthermore, assume that the samples are independent from each other.

As mentioned above, since the conditional ROC curve is given in equation (4), an estimation procedure can be obtained following the next steps: i) compute estimators of the regression functions and variance parameters, ii) calculate the corresponding residuals and replace the distribution and quantile functions, G_D and G_H^{-1} , by suitable estimators

and iii) plug-in estimators of the regression functions and variance parameters in (4).

In order to obtain a final robust estimator of the ROC and AUC curves, it is necessary to consider robust estimators not only in the first step of the described procedure, but also in the second one. In fact, if robust estimators are only considered for the estimation of the regression and variance functions, large residuals would influence the classical empirical distribution and quantile function estimators wasting the efforts made in the first step to get robustness. Taking these ideas into account, we propose the following stepwise procedure:

Step 1. Estimate $\mu_{0,H}(\mathbf{x})$, $\sigma_{0,H}$, $\mu_{0,D}(\mathbf{x})$, $\sigma_{0,D}$ in a robust fashion from the samples $(y_{H,1}, \mathbf{x}_{H,1}), \dots, (y_{H,n_H}, \mathbf{x}_{H,n_H})$ and $(y_{D,1}, \mathbf{x}_{D,1}), \dots, (y_{D,n_D}, \mathbf{x}_{D,n_D})$, respectively. Denote the resulting estimators by $\hat{\mu}_H(\mathbf{x})$, $\hat{\sigma}_H$, $\hat{\mu}_D(\mathbf{x})$ and $\hat{\sigma}_D$.

Step 2. Compute for each sample the standardized regression residuals

$$r_{H,i} = \frac{y_{H,i} - \hat{\mu}_H(\mathbf{x}_{H,i})}{\hat{\sigma}_H} \quad \text{and} \quad r_{D,i} = \frac{y_{D,i} - \hat{\mu}_D(\mathbf{x}_{D,i})}{\hat{\sigma}_D}.$$

From these residuals, evaluate robust estimators of the distribution and quantile functions, denoted, \hat{G}_D and \hat{G}_H^{-1} , respectively.

Step 3. Plug-in the robust estimators computed in the first two steps into equation (4) to obtain

$$\widehat{\text{ROC}}_{\mathbf{x}}(p) = 1 - \hat{G}_D \left(\frac{\hat{\mu}_H(\mathbf{x}) - \hat{\mu}_D(\mathbf{x})}{\hat{\sigma}_D} + \frac{\hat{\sigma}_H}{\hat{\sigma}_D} \hat{G}_H^{-1}(1 - p) \right).$$

A key point of the above procedure is to provide robust and consistent estimators in the first and second steps. Regarding **Step 1**, the considered regression models (2) and (3) may be either parametric, nonparametric or semiparametric. In each case, suitable robust estimators must be used. In particular, in the parametric case, linear or nonlinear models may be adequate. For instance, when the conditional model is a linear model, the *MM*-estimators introduced in Yohai (1987) are a recommended option, while under a

nonlinear one the weighted MM –estimators presented in Bianco and Spano (2019) may be used.

Beyond the robust estimation of the regression functions and the scales σ_j , it is necessary to detect outliers in order to obtain a robust version of the empirical distribution and quantile function estimators. Unlike the classical empirical estimators, where all the observations have the same weight, downweighting in the second step atypical points, i.e., those values that lie far away from the bulk of the data, may result in a more resistant procedure.

3.2 Regarding the estimation of the residual’s distribution

As in Gervini and Yohai (2002), we consider adaptive weights computed from the empirical distribution of the residuals obtained from a robust fit. To describe the extension of their proposal and to fix ideas, let us consider a general homoscedastic nonlinear regression model. Similar arguments can be consider when the model is fully nonparametric, semiparametric or even heteroscedastic.

Assume that we have a random sample $(y_1, \mathbf{x}_1), \dots, (y_n, \mathbf{x}_n)$, where \mathbf{x}_i is a vector of p explanatory variables and y_i is a response variable that satisfies

$$y_i = \mu(\mathbf{x}_i) + u_i = f(\mathbf{x}_i, \boldsymbol{\beta}_0) + \sigma_0 \epsilon_i, \quad i = 1 \dots n, \quad (5)$$

with $\boldsymbol{\beta} \in \mathbb{R}^q$, σ_0 the scale parameter and f a known function. Note that the dimension of the regression parameter $\boldsymbol{\beta}$ may be equal or not to that of the covariates. The errors ϵ_i are independent and identically distributes (i.i.d.) with unknown distribution G_0 and independent of the covariates \mathbf{x}_i . We will assume that G_0 is symmetric around 0.

Consider robust estimators of regression and scale, let us say $\hat{\mu}(\cdot)$ and $\hat{\sigma}$, and compute standardized residuals $r_i = (y_i - \hat{\mu}(\mathbf{x}_i))/\hat{\sigma}$. In particular, under the nonlinear regression model (5), $\hat{\mu}(\mathbf{x}_i) = f(\mathbf{x}_i, \hat{\boldsymbol{\beta}})$, where for instance, $\hat{\boldsymbol{\beta}}$ is an S – or an MM –estimator. On

the basis of these residuals, the classical empirical distribution at point t can be computed as $\hat{G}_{n,\text{EMP}}(t) = (1/n) \sum_{i=1}^n \mathbb{I}_{r_i \leq t}$. Large values of $|r_i|$ suggest that the corresponding pairs (y_i, \mathbf{x}_i) may be outliers. In that case, under a normal error model, it seems wise to consider as atypical those points whose residuals are larger than a certain cut-off value t^* , that is, such that $|r_i| > t^*$. Typically, t^* is chosen as 2.5 by taking the standard normal distribution as a benchmark. To take into account these considerations, weighting may be a useful alternative in the computation of the empirical distribution estimator. However, in order to make the cut-off criterion more flexible and more data-driven, adaptive cut-off values could be considered in this process.

We compute the adaptive weighted empirical distribution at point t as:

$$\hat{G}_n(t) = \frac{1}{\sum_{\ell=1}^n w_\ell} \sum_{i=1}^n w_i \mathbb{I}_{r_i \leq t}, \quad (6)$$

where the weights $w_i \geq 0$ are based on a weight function $w : \mathbb{R} \rightarrow [0, 1]$ non-increasing, right continuous, continuous in a neighbourhood of 0, $w(0) = 1$, $w(u) > 0$ for $0 < u < 1$ and $w(u) = 0$ for $u \geq 1$. The fact that $w(u) = 0$ for $u \geq 1$ ensures that $w_i = 0$ when $|r_i|$ is larger than the selected cut-off value, so, as mentioned in Gervini and Yohai (2002), observations with large residuals are completely eliminated in the weighted estimators.

To define the adaptive cut-off values, consider the empirical distribution function of the absolute standardized residuals r_i given by

$$G_n^+(t) = \frac{1}{n} \sum_{i=1}^n \mathbb{I}_{|r_i| \leq t}.$$

and let $G_0^+(t)$ be the distribution of the absolute errors when $\epsilon_i \sim G_0$. As noted in Gervini and Yohai (2002), if for a large t it happens that $G_n^+(t) < G_0^+(t)$, we have that the sample proportion of absolute residuals that exceeds t is greater than the theoretical proportion suggesting that outliers are present among the data.

Since in practice the actual distribution of ϵ_i is unknown, an hypothetical distribution G , such as the standardized normal distribution, is assumed. Gervini and Yohai(2002)

consider as a measure of the percentage of atypical data

$$d_n = \sup_{t \geq 0} \{G^+(t) - G_n^+(t)\}^+ = \sup_{t \geq 0} \{\max(G^+(t) - G_n^+(t), 0)\},$$

where $\{\cdot\}^+$ denotes the positive part, G^+ is the distribution of the random variable $|V|$ when $V \sim G$. Let $|r|_{(1)} \leq |r|_{(2)} \leq \dots \leq |r|_{(n)}$ denote the order statistics of the standardized residuals. As those authors note

$$d_n = \max_{1 \leq i \leq n} \left\{ \max \left(G^+ (|r|_{(i)}) - \frac{(i-1)}{n}, 0 \right) \right\}.$$

Hence, a possible cut-off value may be

$$\bar{t}_n = |r|_{i_n} = \min\{t : G_n^+(t) \geq 1 - d_n\},$$

where $i_n = n - [nd_n]$. However, as noted in Gervini and Yohai (2002), the values of d_n may be large for small values of n even when outliers are not present in the sample. Therefore, to combine high efficiency for small samples we define the threshold value as

$$t_n = \max(\bar{t}_n, \eta), \tag{7}$$

where η is some large quantile of G^+ , that is, $\eta = (G^+)^{-1}(p)$ for some p close to 1.

With this adaptive cut-off value, by means of the weight function $w : \mathbb{R} \rightarrow [0, 1]$, we define

$$w_i = w\left(\frac{r_i}{t_n}\right), \tag{8}$$

and the adaptive weighted empirical distribution as in (6), which allows to define also the weighted quantile function. Appendix B provides some uniform consistency results for the adaptive weighted empirical distribution \widehat{G}_n defined through (6) and (8), under mild conditions.

4 Consistency results

The results in this section are based on those concerning the uniform consistency of the weighted distribution function defined in (6) which are given in Appendix B. We

will consider a general nonlinear regression model, extensions to other settings, such as nonparametric regression models, can be obtained similarly. Henceforth, $(y_{j,i}, \mathbf{x}_{j,i})$, $1 \leq i \leq n_\ell$, for $j = D, H$, stand for independent random samples from the diseased and healthy populations with the same distribution as $(Y_D, \mathbf{X}_D) \in \mathbb{R}^{p+1}$ and $(Y_H, \mathbf{X}_H) \in \mathbb{R}^{p+1}$, respectively, where (Y_D, \mathbf{X}_D) satisfy (2) and (Y_H, \mathbf{X}_H) fulfils (3). The errors $\epsilon_j \sim G_j$ are independent of \mathbf{X}_j , for $j = D, H$. In this situation, using (4), we get that

$$\text{ROC}_{\mathbf{x}}(p) = 1 - G_D \left(\frac{\mu_{0,H}(\mathbf{x}) - \mu_{0,D}(\mathbf{x})}{\sigma_{0,D}} + \frac{\sigma_{0,H}}{\sigma_{0,D}} G_H^{-1}(1-p) \right).$$

To avoid burden notation, for $j = D, H$, we will denote as $\hat{G}_j = \hat{G}_{j,n_j}$ the weighted empirical distribution function defined in (6) using the sample $(y_{j,i}, \mathbf{x}_{j,i})$, $1 \leq i \leq n_j$ and robust consistent estimators $\hat{\mu}_j$ and $\hat{\sigma}_j$ of $\mu_{0,j}$ and $\sigma_{0,j}^2$, respectively. Then, the estimator of the ROC curve whose uniform consistency we will study is given by

$$\widehat{\text{ROC}}_{\mathbf{x}}(p) = 1 - \hat{G}_D \left(\frac{\hat{\mu}_H(\mathbf{x}) - \hat{\mu}_D(\mathbf{x})}{\hat{\sigma}_D} + \frac{\hat{\sigma}_H}{\hat{\sigma}_D} \hat{G}_H^{-1}(1-p) \right).$$

We will need the following assumptions on the errors distributions and on their estimates:

A1 $G_H : \mathbb{R} \rightarrow (0, 1)$ has an associated density g_H such that $g_H(y) > 0$, for all $y \in \mathbb{R}$.

A2 $G_D : \mathbb{R} \rightarrow (0, 1)$ is continuous.

A3 $\|\hat{G}_j - G_j\|_\infty \xrightarrow{a.s.} 0$, $j = D, H$.

A4 For each fixed \mathbf{x} , $|\hat{\mu}_j(\mathbf{x}) - \mu_{0,j}(\mathbf{x})| \xrightarrow{a.s.} 0$, $j = D, H$.

A5 For any compact set $\mathcal{K} \subset \mathcal{S}$, $\sup_{\mathbf{x} \in \mathcal{K}} |\hat{\mu}_j(\mathbf{x}) - \mu_{0,j}(\mathbf{x})| \xrightarrow{a.s.} 0$, $j = D, H$.

A6 The regression functions $\mu_{0,j}$ are such that, for any compact set \mathcal{K} $\sup_{\mathbf{x} \in \mathcal{K}} |\mu_{0,j}(\mathbf{x})| = A_j < \infty$.

Remark 1. If we are dealing with a parametric regression model, i.e., when $\mu_{0,D}(\mathbf{x}) = f_D(\mathbf{x}, \beta_{0,D})$ and $\mu_{0,H}(\mathbf{x}) = f_H(\mathbf{x}, \beta_{0,H})$ and $\hat{\beta}_j$ and $\hat{\sigma}_j$ stand for robust consistent estimators of $\beta_{0,j}$ and $\sigma_{0,j}^2$, respectively, the estimator of the ROC curve equals

$$\widehat{ROC}_{\mathbf{x}}(p) = 1 - \hat{G}_D \left(\frac{f_H(\mathbf{x}, \hat{\beta}_H) - f_D(\mathbf{x}, \hat{\beta}_D)}{\hat{\sigma}_D} + \frac{\hat{\sigma}_H}{\hat{\sigma}_D} \hat{G}_H^{-1}(1 - p) \right).$$

In this framework, conditions under which **A3** holds for the linear model $f_j(\mathbf{x}, \beta_{0,j}) = \mathbf{x}^T \beta_{0,j}$ or more generally, for a nonlinear model are given in the Appendix B. The derivation of conditions that guarantee the validity **A3** under nonparametric or semiparametric models are beyond the scope of this paper.

On the other hand, **A4** to **A6** hold if the non-linear regression functions are such that

A7 For each fixed \mathbf{x} , the regression functions $f_j(\mathbf{x}, \mathbf{b})$ are continuous in \mathbf{b} .

A8 The functions f_j are such that, for any compact set \mathcal{K} and any sequence $\beta_n \rightarrow \beta_{0,j}$, we have $\sup_{\mathbf{x} \in \mathcal{K}} |f_j(\mathbf{x}, \beta_n) - f_j(\mathbf{x}, \beta_{0,j})| \rightarrow 0$. Further, $\sup_{\mathbf{x} \in \mathcal{K}} |f_j(\mathbf{x}, \beta_j)| = A_j < \infty$.

In particular, these assumptions hold if the regression model is a linear one.

Theorem 1. Let $(y_{j,i}, \mathbf{x}_{j,i})$, $1 \leq i \leq n_j$, $j = D, H$, be independent observations satisfying (2) and (3), respectively and assume that $\hat{\mu}_j$ and $\hat{\sigma}_j$ are strongly consistent estimators of $\mu_{0,j}$ and $\sigma_{0,j}$, respectively. Then, under **A1** to **A3** and **A4**,

(i) $\sup_{0 < p < 1} |\widehat{ROC}_{\mathbf{x}}(p) - ROC_{\mathbf{x}}(p)| \xrightarrow{a.s.} 0$.

(ii) If, in addition, **A5** holds, G_D has a bounded density g_D and the regression functions $\mu_{0,j}$ satisfy **A6**, then, for any $\delta > 0$ $\sup_{\delta < p < 1 - \delta} \sup_{\mathbf{x} \in \mathcal{K}} |\widehat{ROC}_{\mathbf{x}}(p) - ROC_{\mathbf{x}}(p)| \xrightarrow{a.s.} 0$.

(iii) Furthermore, assume that G_D has a bounded density g_D , the regression functions $\mu_{0,j}$ satisfy **A6** and the conditional ROC function is such that, for any $\epsilon > 0$, there exists $0 < \eta < 1$ such that, for any $\mathbf{x} \in \mathcal{K}$, $ROC_{\mathbf{x}}(\eta) < \epsilon$ and $1 - ROC_{\mathbf{x}}(1 - \eta) < \epsilon$, then $\sup_{0 < p < 1} \sup_{\mathbf{x} \in \mathcal{K}} |\widehat{ROC}_{\mathbf{x}}(p) - ROC_{\mathbf{x}}(p)| \xrightarrow{a.s.} 0$.

As a consequence of Theorem 1, we immediately get the following result.

Corollary 1. *Let $(y_{j,i}, \mathbf{x}_{j,i}) \sim (Y_j, \mathbf{X}_j)$, $1 \leq i \leq n_j$, $j = D, H$, be independent observations satisfying*

$$Y_D = f_D(\mathbf{X}_D, \beta_{0,D}) + \sigma_{0,D}\epsilon_D \quad Y_H = f_H(\mathbf{X}_H, \beta_{0,H}) + \sigma_{0,H}\epsilon_H ,$$

where, for $j = D, H$, the errors $\epsilon_j \sim G_j$ are independent of \mathbf{X}_j , for $j = D, H$. Assume that $\hat{\beta}_j$ and $\hat{\sigma}_j$ are strongly consistent estimators of $\beta_{0,j}$ and $\sigma_{0,j}$, respectively. Then, under **A1** to **A7**,

$$(i) \sup_{0 < p < 1} |\widehat{ROC}_{\mathbf{x}}(p) - ROC_{\mathbf{x}}(p)| \xrightarrow{a.s.} 0.$$

(ii) If, in addition, G_D has a bounded density g_D and the regression functions f_j satisfy **A8**, then $\sup_{\mathbf{x} \in \mathcal{K}} |\widehat{ROC}_{\mathbf{x}}(p) - ROC_{\mathbf{x}}(p)| \xrightarrow{a.s.} 0$.

Moreover, for any $\delta > 0$ $\sup_{\delta < p < 1-\delta} \sup_{\mathbf{x} \in \mathcal{K}} |\widehat{ROC}_{\mathbf{x}}(p) - ROC_{\mathbf{x}}(p)| \xrightarrow{a.s.} 0$.

(iii) Furthermore, assume that G_D has a bounded density g_D , the regression functions f_j satisfy **A8** and the conditional ROC function is such that, for any $\epsilon > 0$, there exists $0 < \eta < 1$ such that, for any $\mathbf{x} \in \mathcal{K}$, $ROC_{\mathbf{x}}(\eta) < \epsilon$ and $1 - ROC_{\mathbf{x}}(1 - \eta) < \epsilon$, then $\sup_{0 < p < 1} \sup_{\mathbf{x} \in \mathcal{K}} |\widehat{ROC}_{\mathbf{x}}(p) - ROC_{\mathbf{x}}(p)| \xrightarrow{a.s.} 0$.

It is worth noticing that the requirement $\sup_{\mathbf{x} \in \mathcal{K}} ROC_{\mathbf{x}}(\eta) < \epsilon$ and $\sup_{\mathbf{x} \in \mathcal{K}} 1 - ROC_{\mathbf{x}}(1 - \eta) < \epsilon$ in (iii) is satisfied when **A8** holds and G_H has support on the whole line as stated in **A1**.

5 Monte Carlo study

In this section, we summarize the results of a simulation study conducted to study the small sample performance of the proposal given in Section 3. The goal of this numerical

experiment is two-fold. On the one hand, we want to illustrate the sensitivity of the classical methods to deviations from the central model. On the other hand, we want to evaluate the performance of our robust proposal under different contamination schemes and to compare it with the classical one. For that purpose, we considered different scenarios and contaminations schemes. In all cases, we generate $Nrep = 1000$ datasets of size $n_D = n_H = n = 100$ and $n_D = n_H = n = 200$. To evaluate if the advantages to be observed in the robust procedure depend on linearity, we considered two regression models, a linear and a nonlinear one. Besides, different contaminating schemes are analysed either contaminating one or both populations.

To summarize the discrepancy between the estimator and the true ROC surface, we consider two grids of points: $\mathcal{G}_p = \{p_j\}_{j=1}^{N_p}$ corresponding to equidistant values between 0.01 and 0.99 with step 0.01 and $\mathcal{G}_x = \{x_i\}_{i=1}^{N_x}$ where the net has step 0.05 within the interval $[a, b]$ with $a = -1$ and $b = 1$ for the linear model, while $a = 0$ and $b = 1$ for the nonlinear one. The estimators performance is then evaluated using the mean over replications of

- the Mean Squared Error (MSE) given by

$$MSE = \frac{1}{N_x N_p} \sum_{i=1}^{N_x} \sum_{j=1}^{N_p} \left(\widehat{ROC}_{x_i}(p_j) - ROC_{x_i}(p_j) \right)^2,$$

- a measure inspired on the Kolmogorov distance (KS) calculated as

$$KS = \sup_{1 \leq i \leq N_x} \sup_{1 \leq j \leq N_p} \left| \widehat{ROC}_{x_i}(p_j) - ROC_{x_i}(p_j) \right|,$$

that give a global summary of the mismatch between the estimated ROC curves and the true ones.

5.1 Numerical study under a linear model

In the first scenario, we consider different homoscedastic linear-mean regression models for the two populations. We considered the same conditions as in Inácio de Carvalho *et al.* (2013), that is, following the linear regression models

$$y_{D,i} = 2 + 4x_{D,i} + \sigma_D \epsilon_{D,i} \quad (9)$$

$$y_{H,i} = 0.5 + x_{H,i} + \sigma_H \epsilon_{H,i} , \quad (10)$$

for all $i = 1, \dots, n$ $\epsilon_{j,i} \sim N(0, 1)$ are independent and independent from $x_{j,i} \sim U(-1, 1)$, for $j = D, H$, $\sigma_D = 2$ and $\sigma_H = 1.5$. Besides, the sample from one population was generated independently from the other one.

Figure 2 displays the surface corresponding to the true ROC curves generated under the central model given by equations (9) and (10).

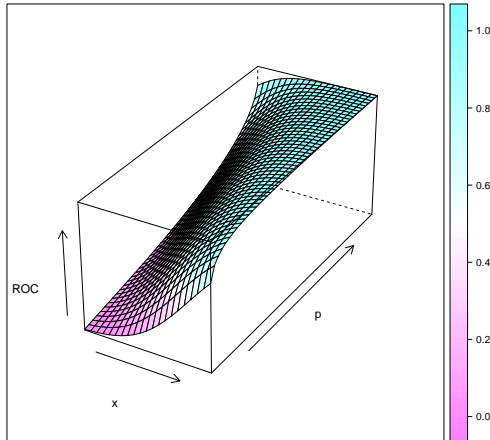


Figure 2: True ROC surface under the central model given by equations (9) and (10) under the linear model.

To evaluate the sensitivity of the classical conditional ROC curve and the robust proposal given in Section 3, we consider different contamination schemes by varying the

sample where we introduce atypical points, the percentage of anomalous data and the size of the outliers.

- C_δ^H : is a contamination in the healthy sample introduced so as to affect the estimation of quantiles of the healthy population. In order to introduce atypical observations, we generate *shift outliers* as follows. The first $m = n\delta$ observations in the healthy dataset were replaced by observations following the model $y_{H,i} = 0.5 + x_{H,i} + S\sigma_H + \sigma_H\epsilon_{H,i}$, where the shift $S \in \mathcal{S} = \{2.5, 5, 7.5, 10, 12.5, 15, 17.5, 20\}$.
- C_δ^D : corresponds to contaminating the diseased population introduced so as to affect the estimation of the empirical distribution of the diseased population. The atypical observations are introduced in the same fashion as in C_δ^H , that is, the first $m = n\delta$ observations in the diseased dataset were replaced by observations following the model $y_{D,i} = 0.5 + x_{D,i} + S\sigma_D + \sigma_D\epsilon_{D,i}$, where the shift $S \in \mathcal{S}$.
- C_δ : we generate now *shift outliers* in both samples simultaneously. For this end, the first $m = n\delta$ observations in each dataset were replaced by observations generated as follows

$$y_{D,i} = 2 + 4x_{D,i} + 20\sigma_D + \sigma_D\epsilon_{D,i} \quad (11)$$

$$y_{H,i} = 0.5 + x_{H,i} + 15\sigma_H + \sigma_H\epsilon_{H,i}, \quad (12)$$

We choose two possible contaminating percentages $\delta = 0.05$ and 0.10 , that is, a 5% or a 10% of observations are modified, respectively. To avoid burden notation, in all Figures and Tables, C_0 stands for the situation of clean samples.

To illustrate the behaviour of the ROC curves for clean and contaminated samples, Figure 3 shows the estimated surfaces obtained with the classical and robust estimators from one of the clean samples generated when $n = 100$ and when the same sample is corrupted with the shifted outliers generated as in equations (11) and (12). The estimators

of the conditional ROC curves were computed on the net of points \mathcal{G}_x and quantiles \mathcal{G}_p , described above. The right panel in Figure 3 illustrates the stability of the proposed method, since the three figures on the right panel are quite similar. On the other hand, the classical estimators are distorted in the presence of outliers, the surface being shifted towards 1 in the central region and flatten towards 0 specially under $C_{0.10}$.

To evaluate the effect of the considered contaminations, Tables 1 to 4, report the summary measures under C_δ^H and C_δ^D for $\delta = 0.05, 0.10$ and $n = 100, 200$. It is worth noticing that MSE and KS take values between 0 and 1 and in this range, large deviations correspond to values close to 1. The reported results show that the classical procedure to estimate the ROC curve is seriously affected by the introduced outliers. It should be taken into account that since the ROC curve varies between 0 and 1, the magnitude of the effect is not as evident as in other settings such as in linear regression models. However, when $n = 100$, under $C_{0.05}^H$, the MSE is 5.5 larger when $S = 20$ than for clean samples, while the robust procedure remains stable. This effect is more striking in Figures 4 and 5 which show the plot of the MSE as a function of the level shift S when $n = 100$ and 200 and for the two contamination percentages. The red and blue lines correspond to the classical and robust proposed methods, respectively. Even though a slight influence is observed for the robust procedure under mild outliers ($S = 2.5$), which are those more difficult to detect, the whole curve is stable when varying S , while the MSE of the classical method quickly increases with the level shift.

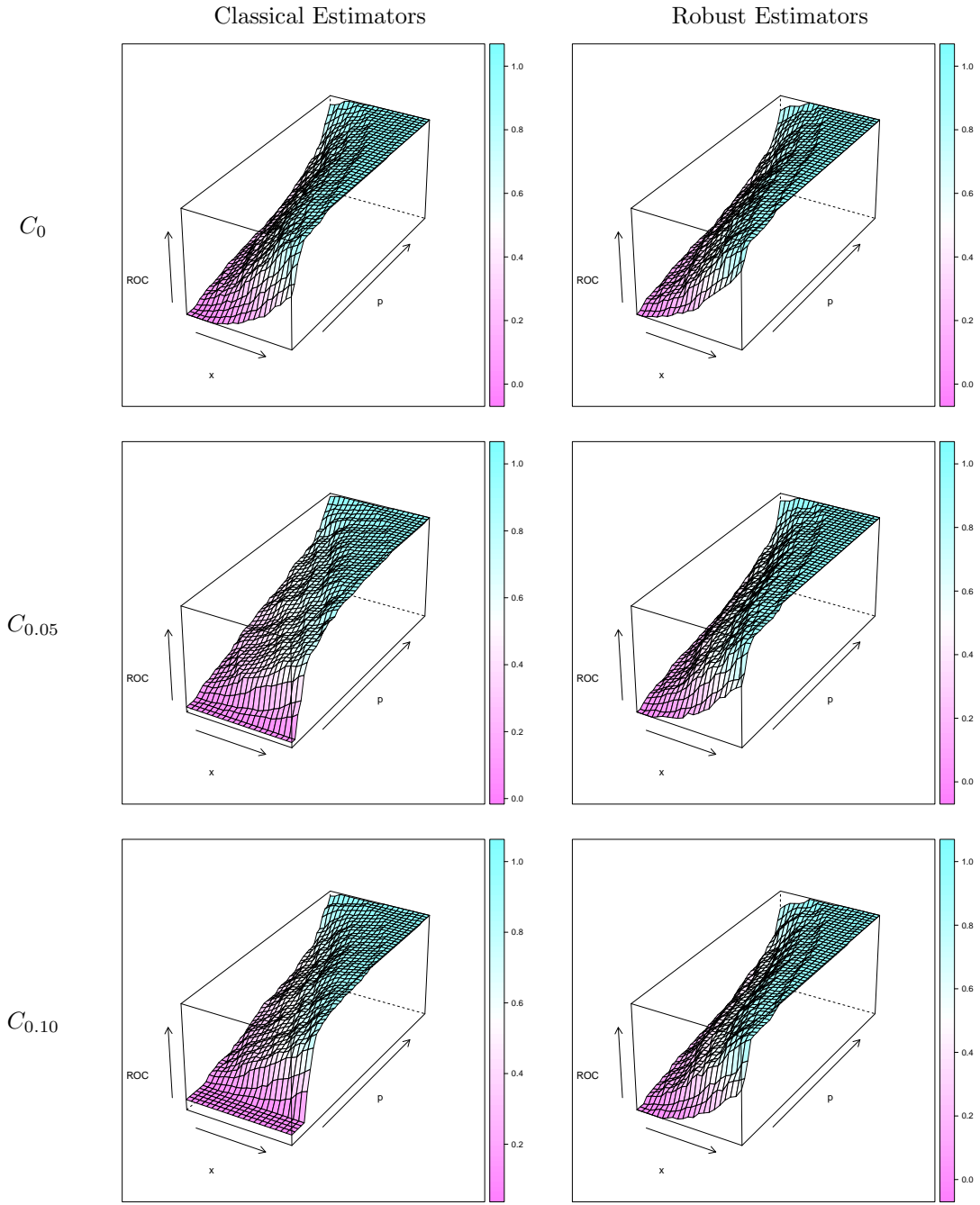


Figure 3: Estimated surfaces for $n_D = n_H = 100$ under the linear model (9) and (10) for a clean and contaminated sample.

			S							
	Method	C_0	2.5	5	7.5	10	12.5	15	17.5	20
			$C_{0.05}^H$							
MSE	Robust	0.0036	0.0040	0.0037	0.0037	0.0037	0.0037	0.0037	0.0037	0.0037
	Classical	0.0032	0.0049	0.0099	0.0114	0.0122	0.0133	0.0145	0.0160	0.0176
KS	Robust	0.1988	0.2156	0.2085	0.2054	0.2056	0.2024	0.2016	0.2016	0.2016
	Classical	0.1949	0.3567	0.7172	0.8189	0.8256	0.8256	0.8256	0.8257	0.8258
			$C_{0.05}^D$							
MSE	Robust	0.0036	0.0039	0.0038	0.0038	0.0039	0.0039	0.0039	0.0039	0.0039
	Classical	0.0032	0.0038	0.0045	0.0055	0.0067	0.0082	0.0098	0.0117	0.0137
KS	Robust	0.1988	0.2041	0.2035	0.2034	0.2037	0.2040	0.2040	0.2040	0.2040
	Classical	0.1949	0.2007	0.2130	0.2279	0.2457	0.2640	0.2829	0.3015	0.3196

Table 1: Sensitivity to the shift size S for $C_{0.05}^H$ and $C_{0.05}^D$ when $n = 100$.

			S							
	Method	C_0	2.5	5	7.5	10	12.5	15	17.5	20
			$C_{0.10}^H$							
MSE	Robust	0.0036	0.0058	0.0041	0.0038	0.0038	0.0038	0.0038	0.0038	0.0038
	Classical	0.0032	0.0086	0.0228	0.0277	0.0297	0.0317	0.0340	0.0365	0.0393
KS	Robust	0.1988	0.2727	0.2411	0.2128	0.2128	0.2128	0.2128	0.2128	0.2128
	Classical	0.1949	0.4406	0.7832	0.8834	0.8946	0.8985	0.9007	0.9013	0.9015
			$C_{0.10}^D$							
MSE	Robust	0.0036	0.0048	0.0042	0.0041	0.0041	0.0041	0.0041	0.0041	0.0041
	Classical	0.0032	0.0052	0.0064	0.0080	0.0100	0.0123	0.0149	0.0176	0.0204
KS	Robust	0.1988	0.2135	0.2085	0.2083	0.2083	0.2083	0.2083	0.2083	0.2083
	Classical	0.1949	0.2125	0.2306	0.2522	0.2761	0.2998	0.3229	0.3450	0.3652

Table 2: Sensitivity to the shift size S for $C_{0.10}^H$ and $C_{0.10}^D$ when $n = 100$.

			S							
	Method	C_0	2.5	5	7.5	10	12.5	15	17.5	20
			$C_{0.05}^H$							
MSE	Robust	0.0017	0.0021	0.0017	0.0017	0.0017	0.0017	0.0017	0.0017	0.0017
	Classical	0.0015	0.0031	0.0083	0.0095	0.0099	0.0104	0.0110	0.0117	0.0125
KS	Robust	0.1380	0.1654	0.1463	0.1419	0.1422	0.1413	0.1411	0.1411	0.1411
	Classical	0.1363	0.3248	0.7169	0.8207	0.8256	0.8256	0.8256	0.8256	0.8256
			$C_{0.05}^D$							
MSE	Robust	0.0017	0.0019	0.0018	0.0018	0.0018	0.0018	0.0018	0.0018	0.0018
	Classical	0.0015	0.0020	0.0023	0.0028	0.0034	0.0042	0.0051	0.0061	0.0073
KS	Robust	0.1380	0.1428	0.1407	0.1406	0.1407	0.1408	0.1408	0.1408	0.1408
	Classical	0.1363	0.1434	0.1514	0.1627	0.1759	0.1903	0.2049	0.2199	0.2349

Table 3: Sensitivity to the shift size S for $C_{0.05}^H$ and $C_{0.05}^D$ when $n = 200$.

			S							
	Method	C_0	2.5	5	7.5	10	12.5	15	17.5	20
			$C_{0.10}^H$							
MSE	Robust	0.0017	0.0040	0.0020	0.0018	0.0018	0.0018	0.0018	0.0018	0.0018
	Classical	0.0015	0.0069	0.0211	0.0253	0.0265	0.0276	0.0288	0.0301	0.0316
KS	Robust	0.1380	0.2470	0.1831	0.1465	0.1465	0.1465	0.1465	0.1465	0.1465
	Classical	0.1363	0.4269	0.7829	0.8845	0.8937	0.8981	0.9008	0.9012	0.9013
			$C_{0.10}^D$							
MSE	Robust	0.0017	0.0028	0.0020	0.0020	0.0020	0.0020	0.0020	0.0020	0.0020
	Classical	0.0015	0.0032	0.0040	0.0048	0.0060	0.0073	0.0089	0.0106	0.0124
KS	Robust	0.1380	0.1585	0.1461	0.1458	0.1458	0.1458	0.1458	0.1458	0.1458
	Classical	0.1363	0.1620	0.1766	0.1930	0.2109	0.2296	0.2482	0.2662	0.2842

Table 4: Sensitivity to the shift size S for $C_{0.10}^H$ and $C_{0.10}^D$ when $n = 200$.

Tables 5 summarizes the results obtained when both samples are contaminated. As above, the reported results correspond to the mean of MSE and KS over 1000 replications. As when contaminating only one population, the mean over replications of MSE for the classical procedure is clearly enlarged under C_δ , while those corresponding to the robust procedure are stable for shifted outliers. It should be noticed that, when considering the discrepancy measure KS of the classical procedure, the median over replications under $C_{0.05}$ equals 0.7756 when the sample size is $n = 100$ and the Absolute Median Deviation (MAD) is 0, meaning that for more than half of the samples the obtained global measure equals 0.7756, which is close to the maximal possible value. This behaviour is also reflected in Figure 6 that shows the boxplots of KS for $n = 100$ and $n = 200$. The boxplot of the classical estimator is completely shifted away under contamination attaining values close to 0.8.

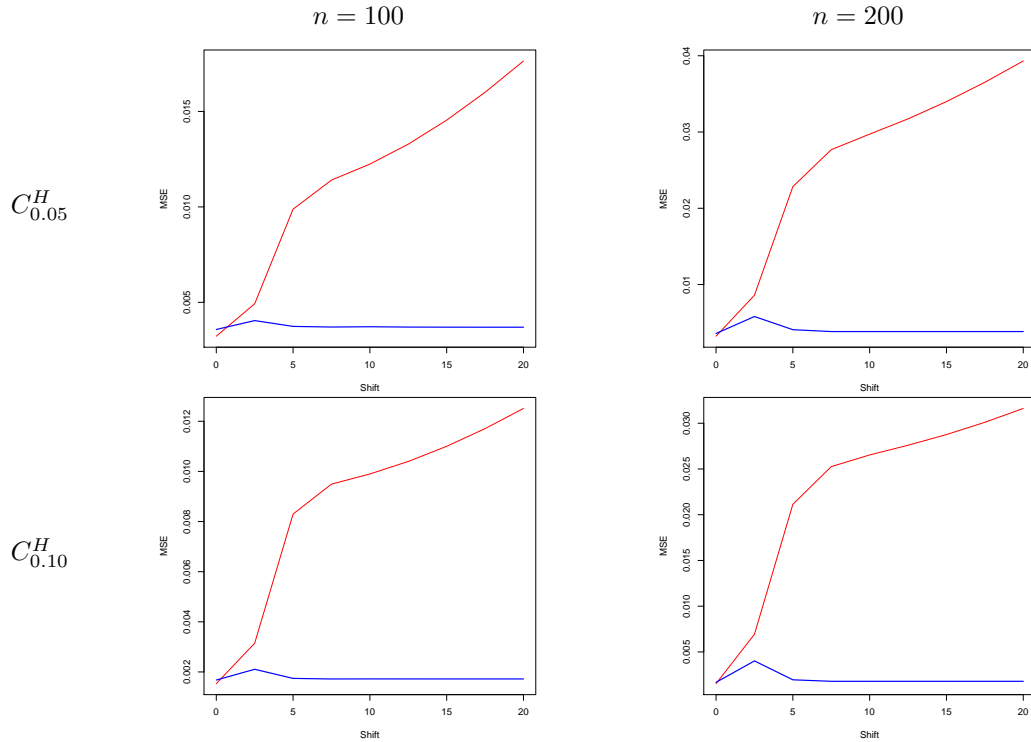


Figure 4: Sensitivity to shift size S : MSE under C_δ^H when $n_D = n_H = 100$ and $n_D = n_H = 200$ for $\delta = 0.05, 0.10$. The red line corresponds to the classical procedure, while the blue one the robust one.

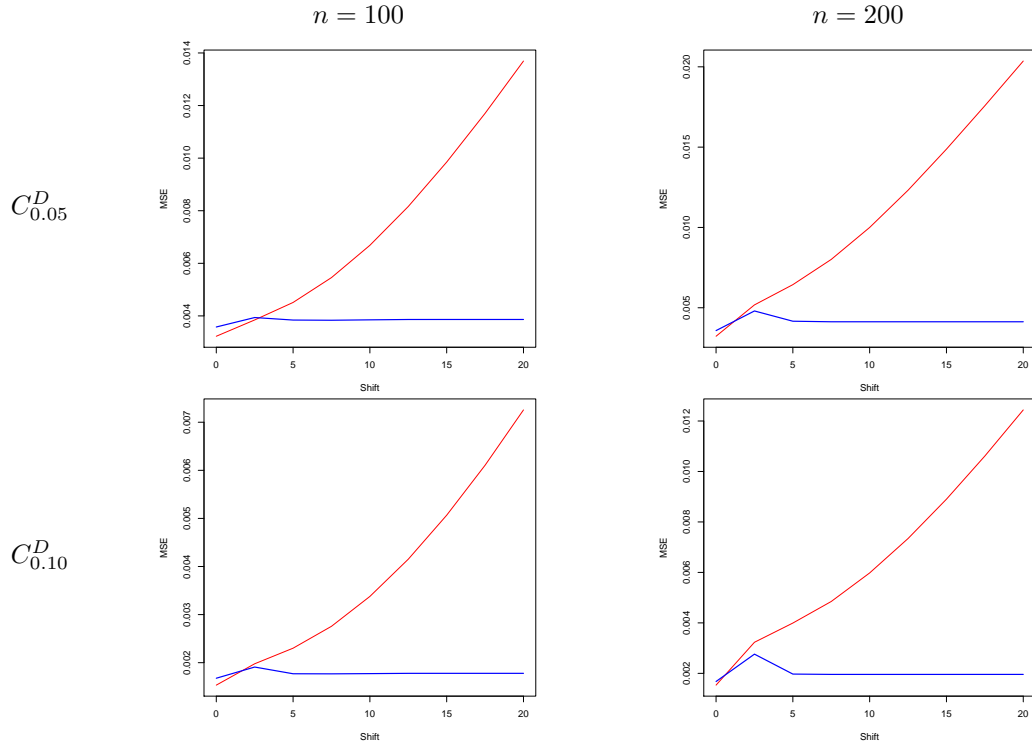


Figure 5: Sensitivity to the shift size S : MSE under C_δ^D when $n_D = n_H = 100$ and $n_D = n_H = 200$ for $\delta = 0.05, 0.10$. The red line corresponds to the classical procedure, while the blue one the robust one.

n		C_0		$C_{0.05}$		$C_{0.10}$	
		Classical	Robust	Classical	Robust	Classical	Robust
100	MSE	0.0032	0.0036	0.0205	0.0040	0.0349	0.0043
	KS	0.1949	0.1988	0.7757	0.2060	0.7993	0.2215
200	MSE	0.0015	0.0017	0.0134	0.0018	0.0269	0.0021
	KS	0.1363	0.1380	0.7756	0.1436	0.7997	0.1538

Table 5: Mean of MSE and KS over replications under the linear model (9) and (10), for clean and samples contaminated as in C_δ .

As mentioned in the Introduction, one of the most popular indices is the *area under the curve*, AUC, which is a summary measure usually considered to evaluate the discriminat-

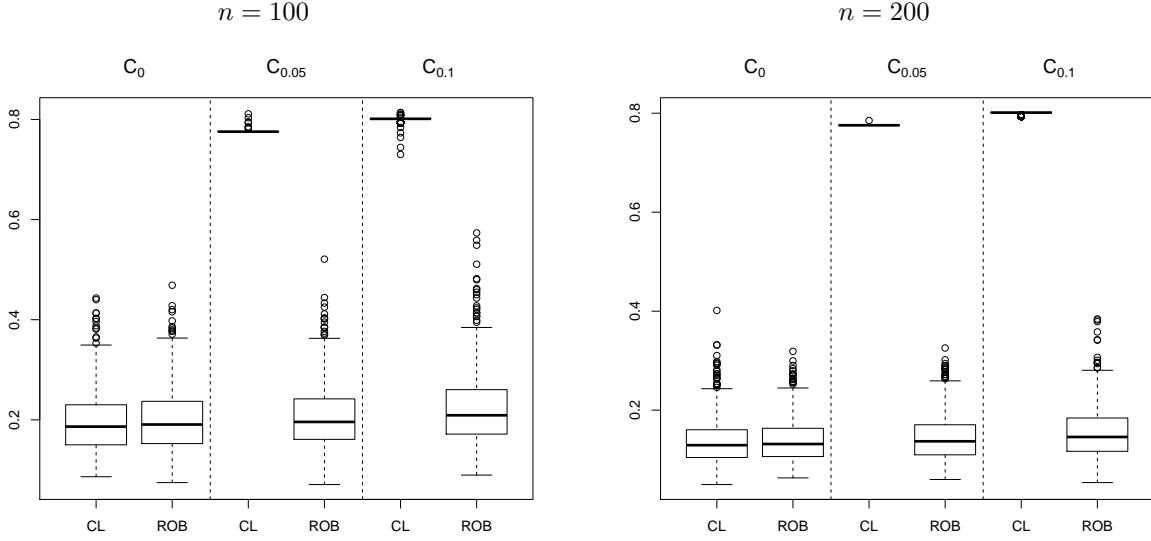


Figure 6: Boxplots of the measure KS obtained from 1000 replications using the classical and robust estimators under the linear model (9) and (10).

ing effect of the biomarker. When covariates are present, the conditional area under the curve is also used as index of the marker accuracy. It is defined as $AUC_x = \int_0^1 ROC_x(p)dp$. Note that in this case, we obtain a single value for each x , hence, the function $x \rightarrow \widehat{AUC}_x$ can be plotted for each sample. Taking into account the observed sensitivity of the classical estimators to outliers, it seems natural that this effect will be inherited by the estimators of the conditional area under the curve, AUC_x . To evaluate this effect, Figures 7 to 10 show the functional boxplots of the estimators \widehat{AUC}_x obtained with the classical and robust procedures, when the sample sizes are $n_H = n_D = 100$, under contaminations C_δ^H and C_δ^D with $\delta = 0.05$ and 0.10 and different values of S . To facilitate comparisons, in Figure 7 we also give the plots corresponding to clean samples. Functional boxplots were introduced by Sun and Genton (2011) and are a useful visualization tool to give a whole picture of the behaviour of a collection of curves. The area in purple represents the 50% inner band of curves, the dotted red lines correspond to outlying curves, the black line indicates the central (deepest) function, while the green line in the plot corre-

sponds to the true AUC_x curve. As shown in Figure 7, when $\delta = 0.05$ and the healthy population is contaminated, the shift causes a bias in the classical estimator of AUC_x , so that the central region of the functional boxplot fails to contain the true function for much of its domain. This effect is more striking when $S = 15$, where also some outlying curves completely distorted appear (see Figure 8). On the other hand, the effect when contaminating the diseased population is not so devastating for the classical procedure. As shown in Figure 9, even though the true curve is not close to the deepest curve it is still within the central region. However, when $S = 20$, the 50% inner band is completely enlarged (see Figure 10). As expected, the robust proposal is stable across the considered contaminations. Moreover, by comparing the upper panel in Figure 7, we observe that the classical and robust estimators of AUC_x are quite similar for clean samples when $n = 100$ and a similar conclusion holds for $n = 200$ (see Figure 12).

Figures 11 and 12 show the functional boxplots of \widehat{AUC}_x for both the classical and robust estimators when the samples are contaminated according to C_δ , when $n = 100$ and $n = 200$, respectively. These figures reveal that the effect of outliers on the classical estimator of the ROC curve is inherited by the estimated area under the curve, which is reflected not only by the presence of a great number of outlying curves, but also by the enlargement of the width of the bars of the functional boxplots, as when contaminating only the diseased population. It should be noted that for $n = 200$ and for values of x in the range $[0.5, 1]$, the true curve is on the limit of the central region. As mentioned above, the robust procedure is stable for the considered contamination. To conclude, these figures make evident the dramatic effect of the introduced outliers on the classical estimates of the area under the ROC curve, while at the same time the robust estimators look very stable.

To have a deeper comprehension of the proposal, it is also of interest to see what would happen if in the stepwise procedure described in Section 3.1, robust estimators were considered only in the first step, i.e., only when computing the regression parameters,

while the usual empirical distribution and quantile function estimators are used in Step 2. The resulting hybrid procedure is illustrated through the functional boxplots of $\widehat{\text{AUC}}_x$ obtained for $n = 100$ and $n = 200$ in Figure 13. These boxplots show that, even when the contamination is less harmful for these estimators than for the classical ones, the true curve lies beyond the functional boxplot 50% inner band of curves when $x \in [0.5, 1]$ and $\delta = 0.05$ and beyond the limits of the functional boxplot when $\delta = 0.10$.

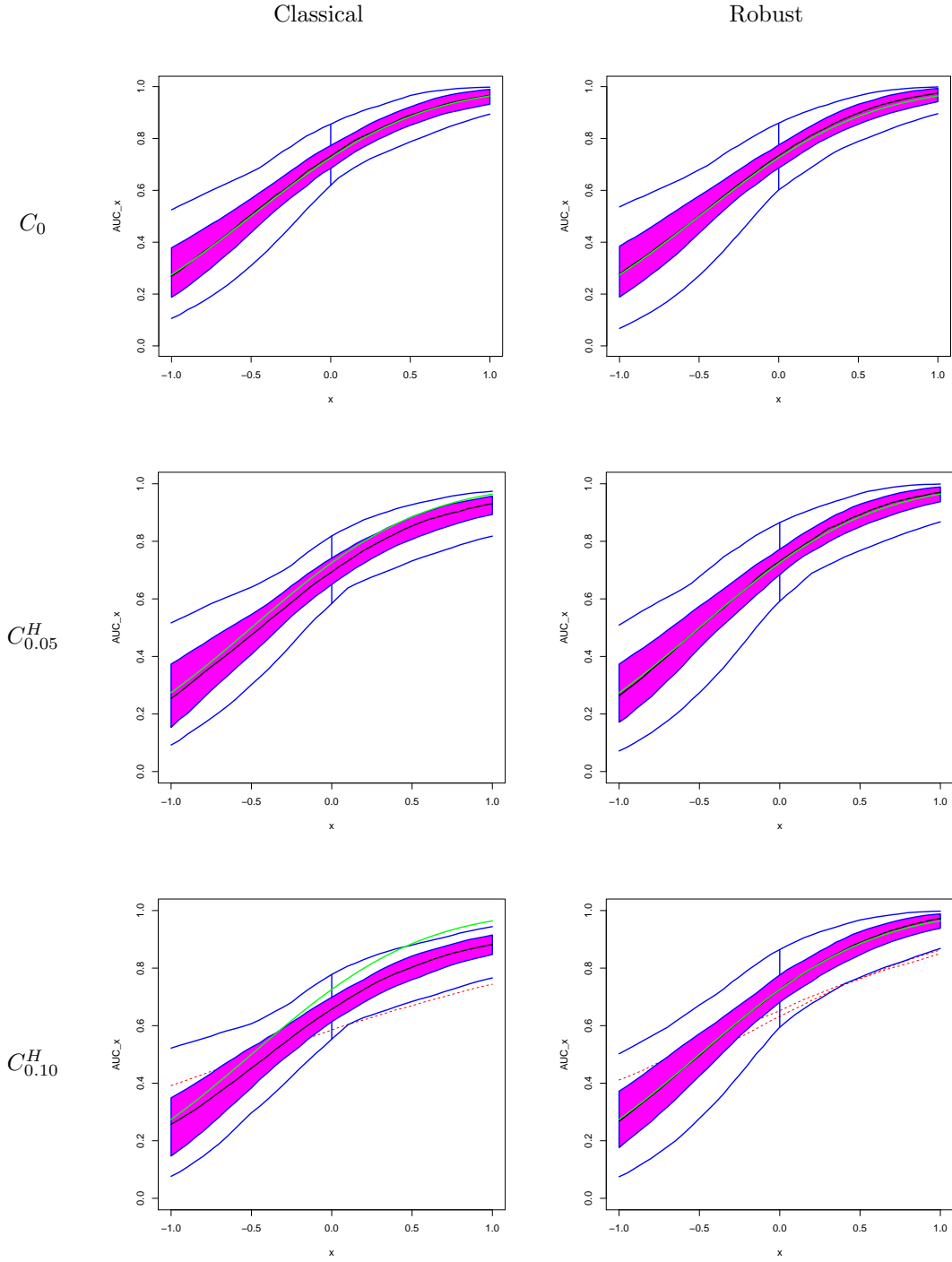


Figure 7: Functional boxplots of \widehat{AUC}_x for $n = 100$ under the linear model (9) and (10) for clean samples and when the samples are contaminated according to C_δ^H for $S = 5$ and $n_H = n_D = 100$. The green line corresponds to the true AUC_x and the dotted red lines to the outlying curves detected by the functional boxplot.

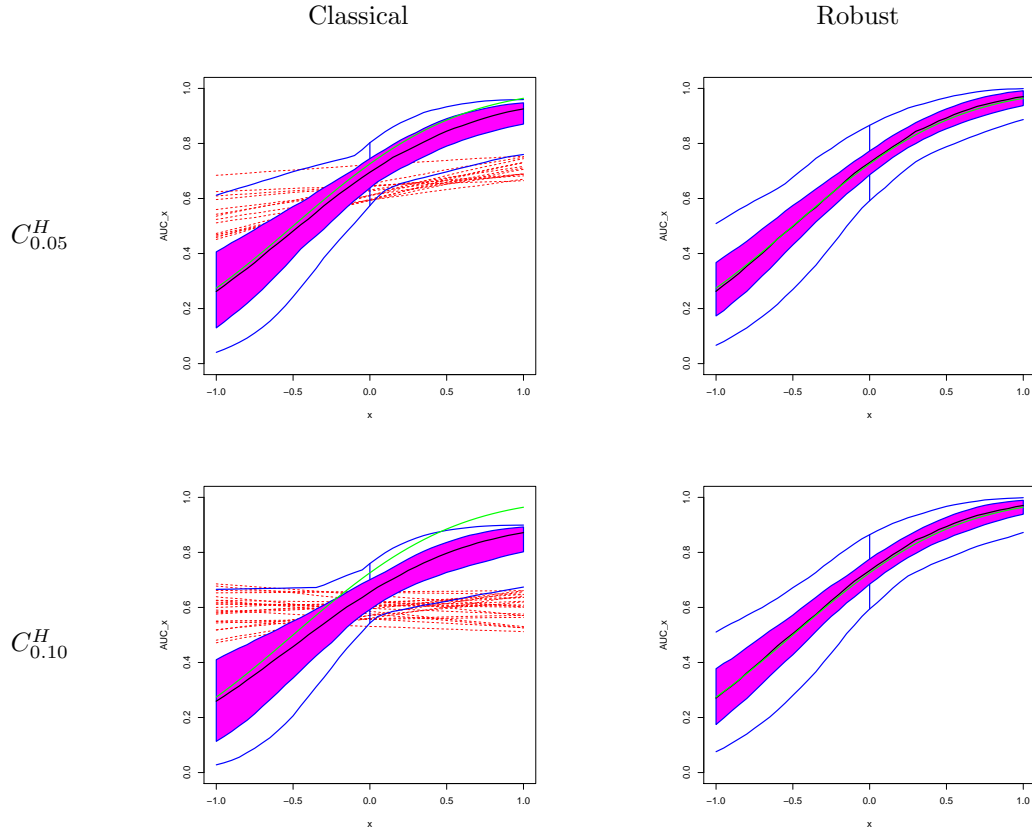


Figure 8: Functional boxplots of $\widehat{\text{AUC}}_x$ for $n = 100$ under the linear model (9) and (10) when the samples are contaminated according to C_δ^H for $S = 15$ and $n_H = n_D = 100$. The green line corresponds to the true AUC_x and the dotted red lines to the outlying curves detected by the functional boxplot.

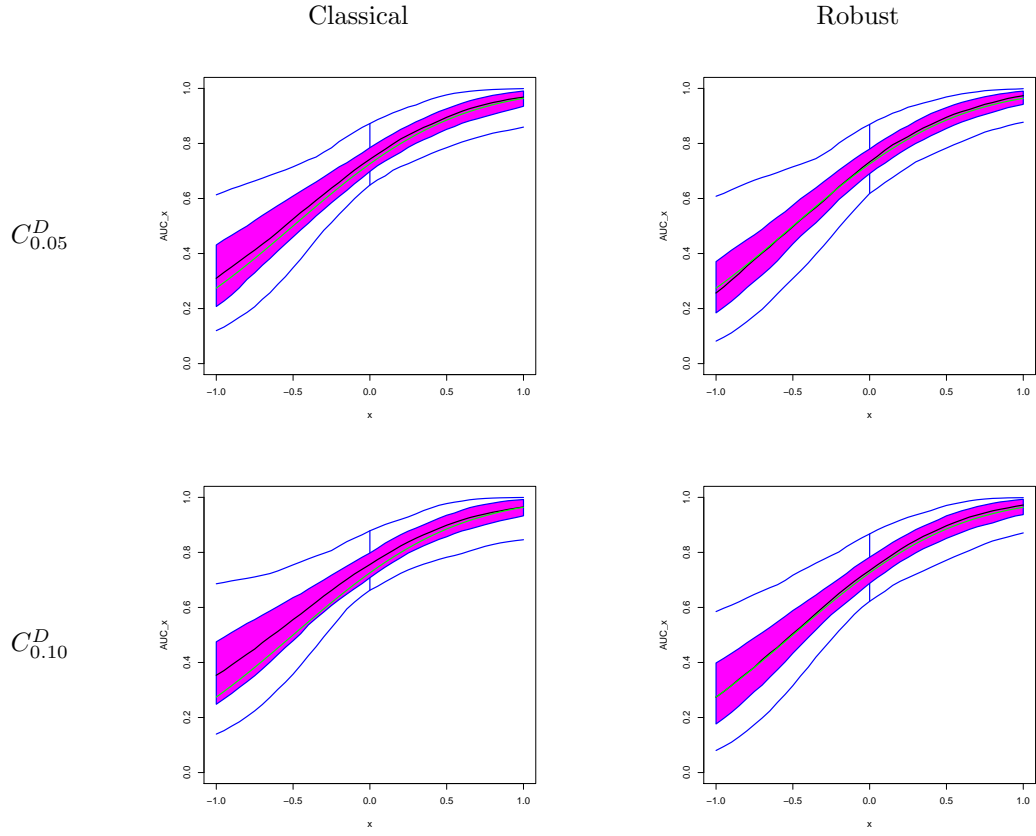


Figure 9: Functional boxplots of $\widehat{\text{AUC}}_x$ for $n = 100$ under the linear model (9) and (10) when the samples are contaminated according to C_{δ}^D for $S = 5$ and $n_H = n_D = 100$. The green line corresponds to the true AUC_x and the dotted red lines to the outlying curves detected by the functional boxplot.

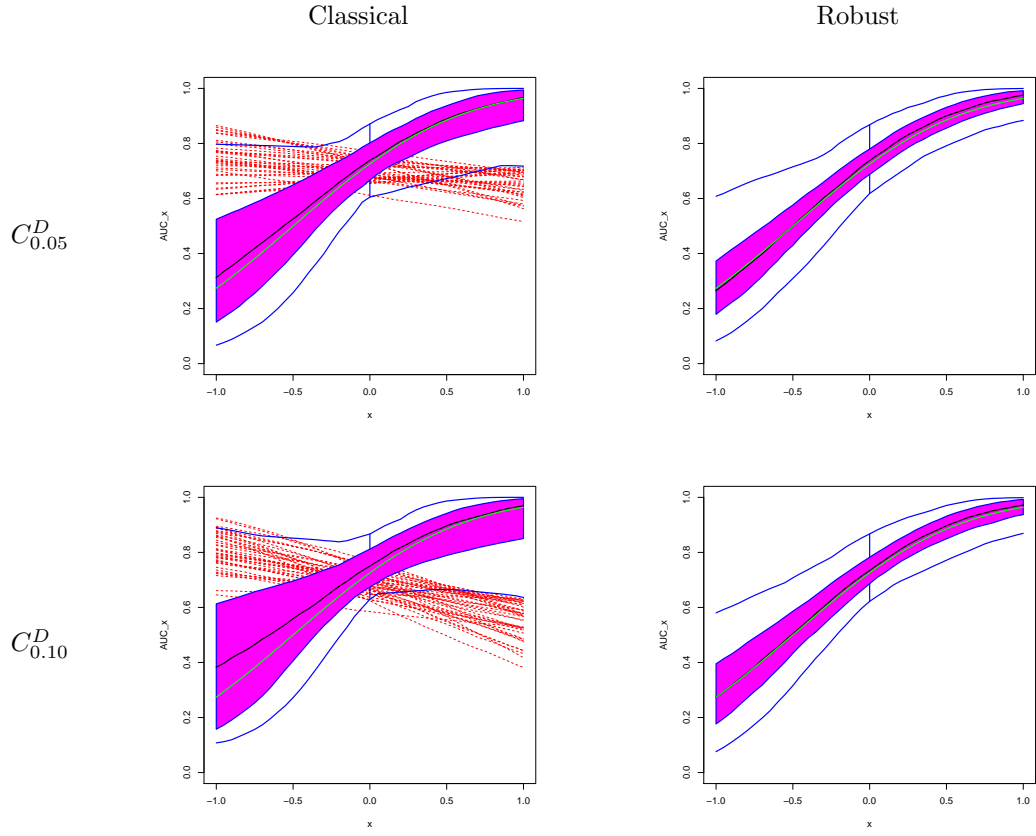


Figure 10: Functional boxplots of \widehat{AUC}_x for $n = 100$ under the linear model (9) and (10) when the samples are contaminated according to C_δ^D for $S = 20$ and $n_H = n_D = 100$. The green line corresponds to the true AUC_x and the dotted red lines to the outlying curves detected by the functional boxplot.

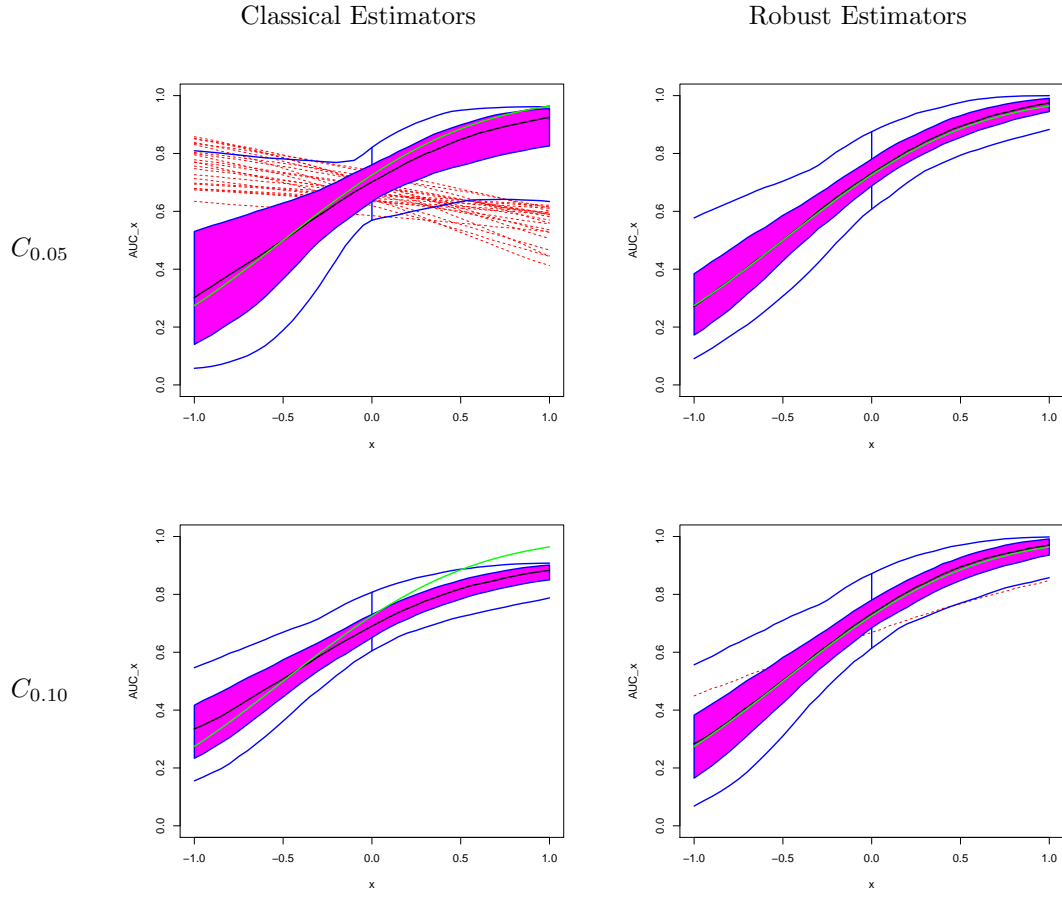


Figure 11: Functional boxplots of \widehat{AUC}_x for $n = 100$, under the linear model (9) and (10) when the samples are contaminated according to C_δ . The green line corresponds to the true AUC_x and the dotted red lines to the outlying curves detected by the functional boxplot.

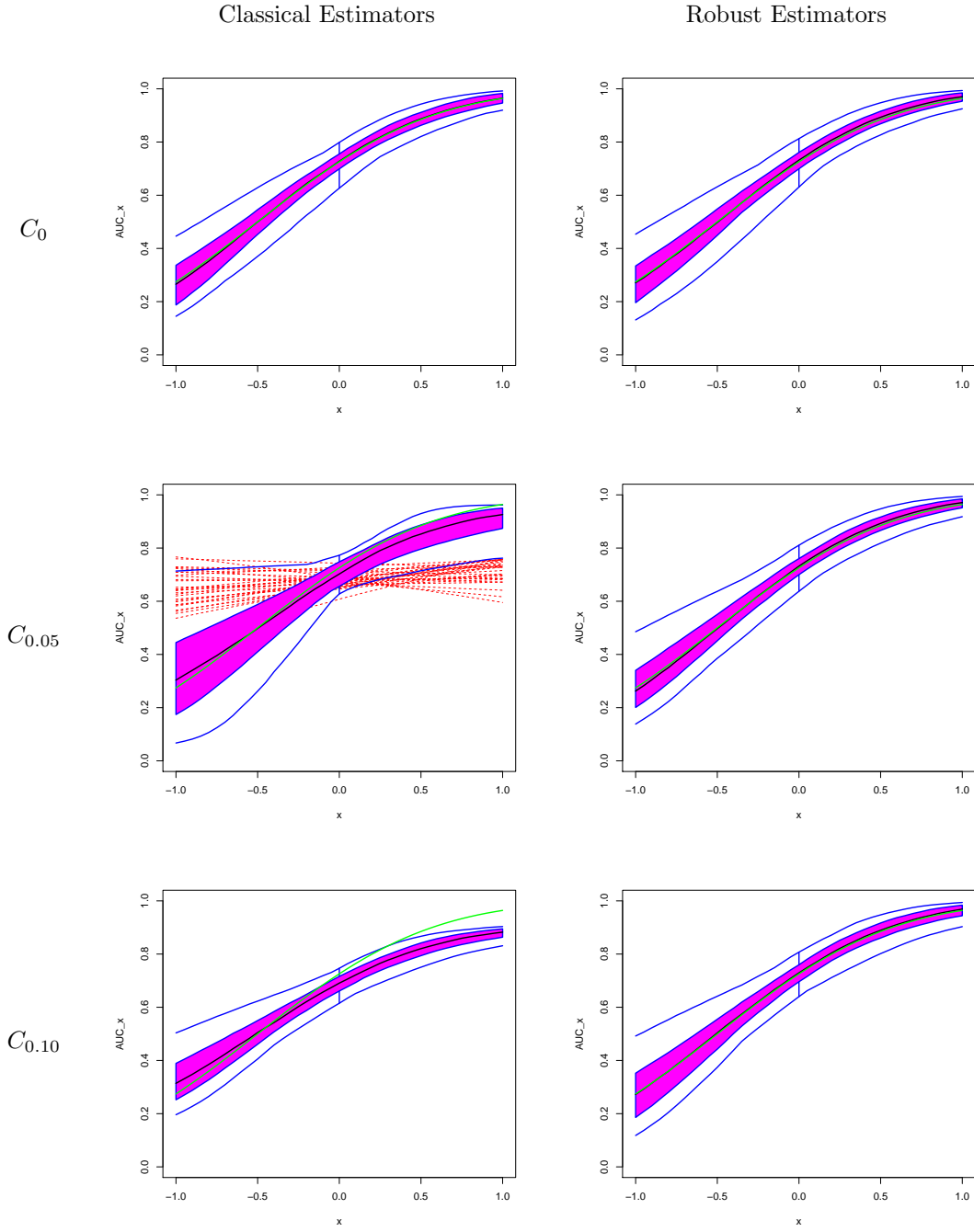


Figure 12: Functional boxplots of \widehat{AUC}_x for $n = 200$, under the linear model (9) and (10) when the samples are contaminated according to C_δ . The green line corresponds to the true AUC_x and the dotted red lines to the outlying curves detected by the functional boxplot.

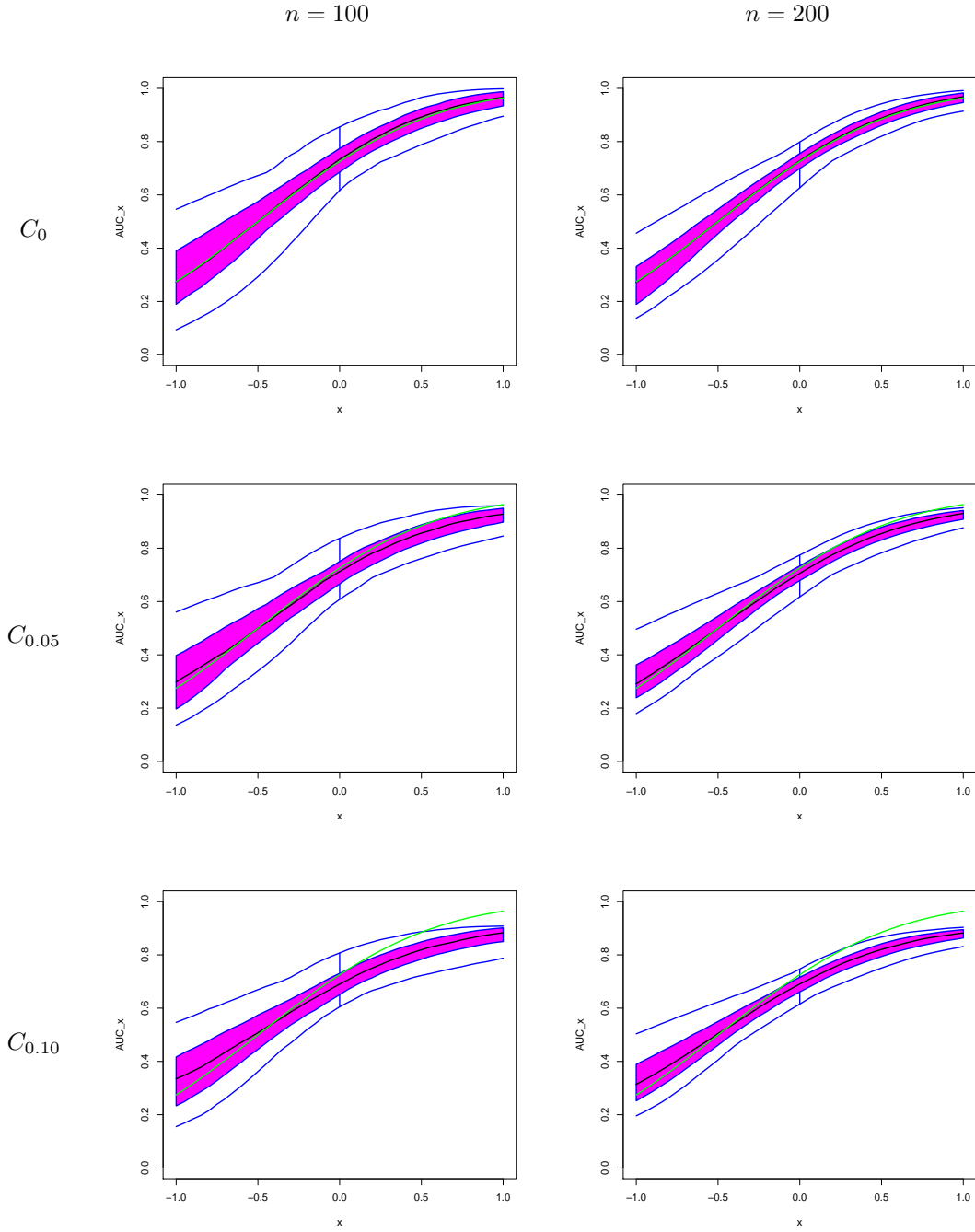


Figure 13: Functional boxplots of \widehat{AUC}_x obtained with the hybrid estimator for $n = 100$ and $n = 200$ with clean samples and under 5% and 10% of contamination under the first linear model. The green line corresponds to the true AUC_x and the dotted red lines to the outlying curves detected by the functional boxplot.

5.2 Numerical study under a non-linear regression model

In this second scenario, we consider an exponential model as in Bianco and Spano (2019), that is, we assume that the observations follow the non-linear regression models

$$y_{D,i} = \beta_{D,1} \exp(\beta_{D,2} x_{D,i}) + \epsilon_{D,i}, \quad (13)$$

$$y_{H,i} = \beta_{H,1} \exp(\beta_{H,2} x_{H,i}) + \epsilon_{H,i}, \quad (14)$$

with $(\beta_{D,1}, \beta_{D,2})^T = (5, 2)$, $(\beta_{H,1}, \beta_{H,2})^T = (3, 1)$ for all $i = 1, \dots, n$ $\epsilon_{j,i} \sim N(0, 1)$ are independent and independent from $x_{j,i} \sim U(0, 1)$, for $j = D, H$. Besides, the sample from one population was generated independently from that of the other one.

In this case, in **Step 1**, the robust regression estimators correspond to the weighted *MM*-estimators defined in Bianco and Spano (2019), while the classical ones to the usual least squares estimators for nonlinear regression models.

To assess the impact of anomalous data on the estimation of the conditional ROC curve, we introduce *shift outliers* in both populations. To explore the sensitivity of the studied methods to the size of the shift, we vary its magnitude. To this end, the first m observations of each sample were replaced by observations following the models

$$y_{D,i} = \beta_{D,1} \exp(\beta_{D,2} x_{D,i}) + z_{D,i} + 0.01\epsilon_{D,i},$$

$$y_{H,i} = \beta_{H,1} \exp(\beta_{H,2} x_{H,i}) + z_{H,i} + 0.01\epsilon_{H,i},$$

where $x_{j,i} \sim U(0.49, 0.5)$ and $\epsilon_{j,i}$ are as above, for $j = D, H$. The shift variables are taken as $z_{j,i} = S + u_{j,i}$, with $S = 2.5, 5, 7.5, 10, 12.5, 15$, $u_{j,i} \sim N(0, 0.01^2)$ for $j = D, H$, $i = 1, \dots, m$.

We consider similar proportions of anomalous points as in Section 5.1, that is, we replace $m = n\delta$ points, $\delta = 0.05$ and 0.10 , which correspond to a 5% or a 10% of replaced observations. As above, we denote this contamination C_δ , while C_0 stands for clean samples. Table 6 summarizes the discrepancy between the true and estimated ROC

curves in terms of the mean over replications of the MSE . The damage of shift outliers on the conditional ROC curve is striking, since the MSE increases more than 10 times when $n = 100$ and more than 20 times when $n = 200$ when S takes the largest values.

				S					
δ	n		C_0	2.5	5	7.5	10	12.5	15
0.05	100	Robust	0.0023	0.0028	0.0023	0.0023	0.0024	0.0024	0.0024
		Classical	0.0019	0.0023	0.0066	0.0127	0.0183	0.0231	0.0269
0.10	100	Robust	0.0023	0.0032	0.0031	0.0024	0.0024	0.0024	0.0024
		Classical	0.0019	0.0029	0.0092	0.0180	0.0240	0.0248	0.0268
0.05	200	Robust	0.0011	0.0018	0.0011	0.0011	0.0011	0.0011	0.0011
		Classical	0.0010	0.0015	0.0062	0.0124	0.0181	0.0229	0.0267
0.10	200	Robust	0.0011	0.0022	0.0014	0.0011	0.0011	0.0011	0.0011
		Classical	0.0010	0.0021	0.0088	0.0178	0.0239	0.0242	0.0249

Table 6: Sensitivity of MSE to the shift size S for C_δ , when $n = 100$ and 200 , under the nonlinear model (13) and (14).

Henceforth, we focus on the particular case of outliers with shift value $S = 10$, a mild value among those considered, so as to have a deeper comprehension of the effect of the introduced anomalous points. Table 7 summarizes the results through the mean of the measures MSE and KS . Note that the mean of the summary measures are distorted for the classical procedure. In particular, when considering the measure KS based on the Kolmogorov distance, the mean is enlarged almost 7 times, under $C_{0.05}$ when $n = 200$.

Figures 14 and 15 show the functionals boxplots of the classical and robust AUC_x obtained for $n = 100$ and $n = 200$, respectively. Notice that in these boxplots, the estimators of conditional area under the curve were plotted in the range $(-0.5, 0.2)$, since for this simulation scheme the AUC_x is almost 1 when the covariate takes values from 0.2 to 0.5. Once again, it becomes evident that the classical estimator suffers from the

introduced contamination and that the classical estimator of AUC_x is completely deviated from the true conditional area under the curve, which is plotted in green, while the robust AUC_x estimator remains very stable.

n		C_0		$C_{0.05}$		$C_{0.10}$	
		Classical	Robust	Classical	Robust	Classical	Robust
100	MSE	0.0019	0.0023	0.0183	0.0024	0.0240	0.0024
	KS	0.1881	0.1944	0.9334	0.2001	0.6893	0.2048
200	MSE	0.0010	0.0011	0.0181	0.0011	0.0239	0.0011
	KS	0.1352	0.1367	0.9364	0.1395	0.7102	0.1445

Table 7: Mean of MSE and KS over replications for clean and contaminated samples, under the nonlinear model (13) and (14), for the level shift $S = 10$.

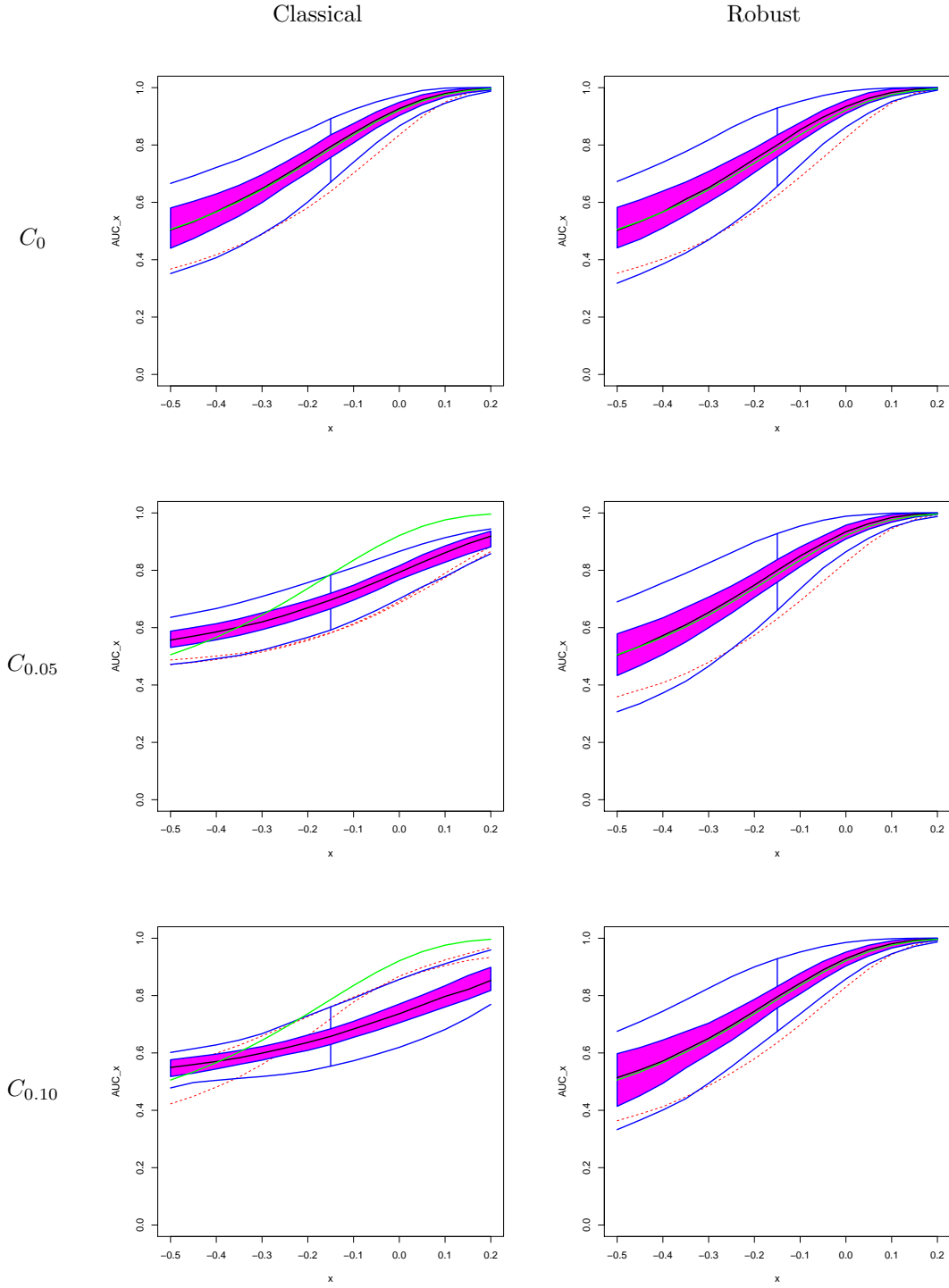


Figure 14: Functional boxplots of \widehat{AUC}_x obtained with the classical and robust estimators for $n = 100$ with clean samples and under 5% and 10% of contamination with level shift $S = 10$, under the nonlinear model (13) and (14). The green line corresponds to the true AUC_x and the dotted red lines to the outlying curves detected by the functional boxplot.

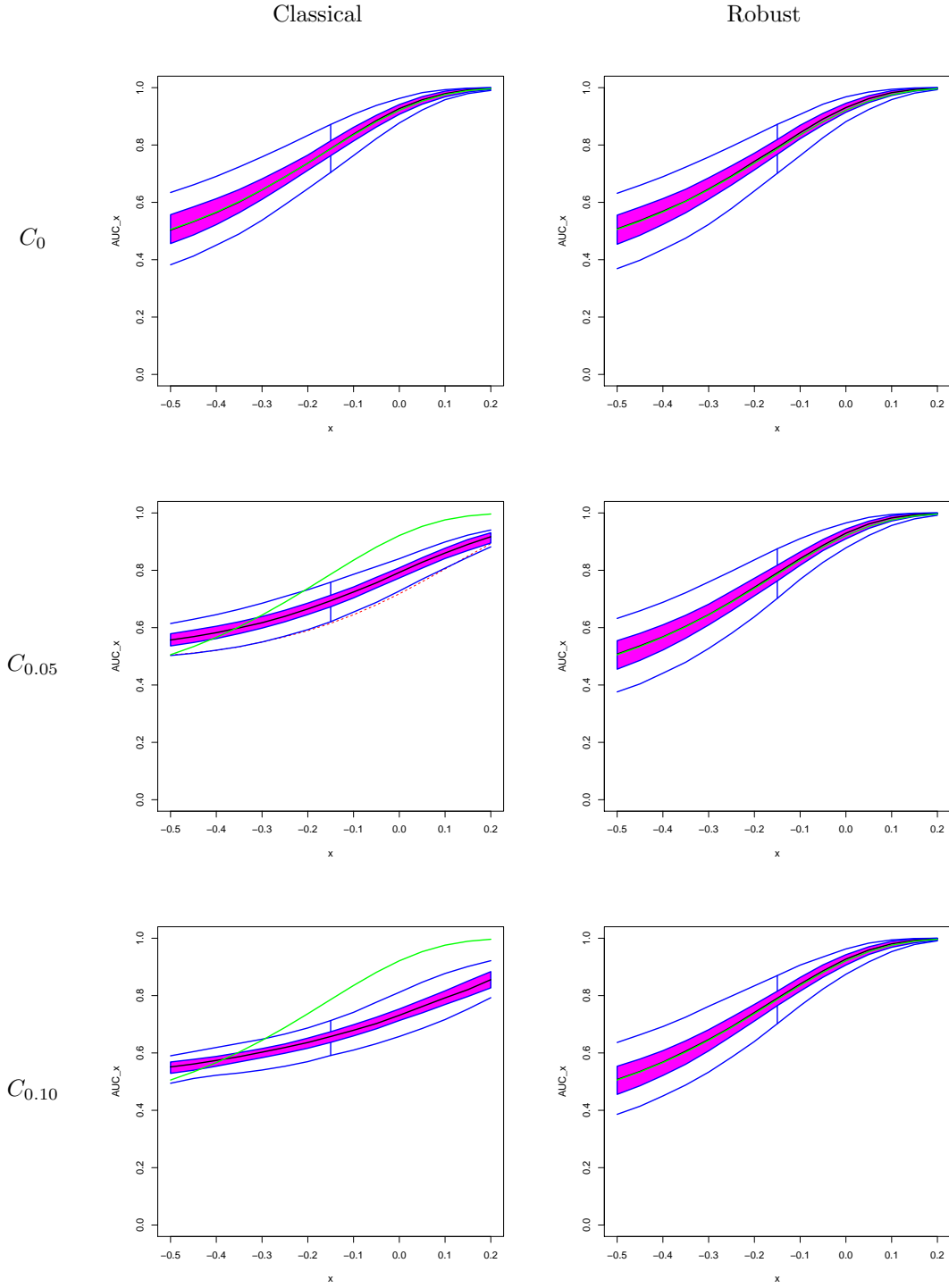


Figure 15: Functional boxplots of \widehat{AUC}_x obtained with the classical and robust estimators for $n = 200$ with clean samples and under 5% and 10% of contamination with level shift $S = 10$, under the nonlinear model (13) and (14). The green line corresponds to the true AUC_x and the dotted red lines to the outlying curves detected by the functional boxplot.

6 Analysis of real data set

In this section, we illustrate the benefits of the robust proposed methodology by means of the diabetes real dataset described in the Introduction.

Following the analysis given in Faraggi (2003), we transform the marker from both populations using power function $f(t) = -t^{-1/2}$. After this, we assume a linear regression model in each population for the transformed marker y , i.e.,

$$\begin{aligned} y_{D,i} &= \beta_{D,1} + \beta_{D,2} x_{D,i} + \epsilon_{D,i}, 1 \leq i \leq 88, \\ y_{H,i} &= \beta_{H,1} + \beta_{H,2} x_{H,i} + \epsilon_{H,i}, 1 \leq i \leq 198, \end{aligned}$$

and we compute the classical and robust estimators of the conditional ROC curves, denoted $\widehat{\text{ROC}}_{\mathbf{x},\text{CL}}$ and $\widehat{\text{ROC}}_{\mathbf{x}}$, respectively. Based on the residuals boxplots of a robust fit, 6 outliers were detected in the healthy sample, labelled as 37, 78, 125, 137, 141 and 150, see the left panel of Figure 16. The filled red points on the central panel of Figure 16 represent the atypical observations encountered in the healthy sample which correspond to vertical outliers. After removing them, the classical estimator of the conditional ROC curves is recomputed with the remaining points, namely $\widehat{\text{ROC}}_{\mathbf{x},\text{CL}}^{(-6)}$. The upper panel of Figure 17 displays the estimated surfaces with these three procedures using equidistant grids of points of size 29 and 28 in p and x , respectively, between $p = 0.01$ and 0.99 and $x = 20$ and 87.5 . In order to facilitate the differences between the estimated surfaces, the middle and lower panel in Figure 17 show the differences between these estimators, making evident that the robust and classical estimator computed without the outliers are very similar all along the studied range, while the classical estimator computed from the whole sample shows a different pattern, clear in the left panel of Figure 17 especially for large values of age.

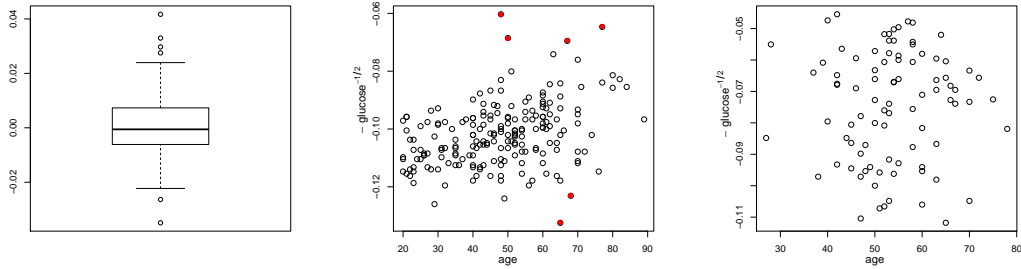


Figure 16: The left panel corresponds to the boxplots of the residuals obtained after a robust fit for healthy sample, while the central and right panels to the scatter plots for the healthy and diseased samples.

7 Final Remarks

The ROC curve is a useful graphical tool that measures the discriminating power of a biomarker to distinguish between two conditions or classes. When the practitioner may measure covariates related to the diagnostic variable which can increase the discriminating power, it is sensible to incorporate them in the analysis. To have a deeper comprehension of the effect of the covariates, it would be advisable to incorporate the covariates information to the ROC analysis instead of considering the marginal ROC curve. Conditional ROC curves may be easily estimated using a plug-in procedure. However, the use of classical regression estimators and empirical distribution and quantile functions may lead to estimates which breakdown in the presence of a small amount of atypical data.

In this piece of work, we introduce a procedure to robustly estimate the conditional ROC curve. The methodology combines robust regression estimators with a weighted empirical distribution function which downweights the effect of large residuals. We prove that the estimators are uniformly strongly consistent under standard regularity conditions. A simulation study shows that our proposed estimators have good robustness and finite-sample statistical properties. Even though our numerical studies focus on a parametric

regression approach, it should be mentioned that our proposal could also be implemented when considering nonparametric or partly parametric regression models, using a robust fit.

Acknowledgment. This work was partially developed while Ana M. Bianco and Graciela Boente were visiting the Departamento de Estadística, Análise Matemática e Optimización de la Universidad de Santiago de Compostela, Spain with the travel support of the program UBAINTE DOCENTES 2019 from the University of Buenos Aires. This research was partially supported by Grants PICT 2018-00740 from ANPCYT and 20020170100022BA from the Universidad de Buenos Aires, Argentina and also by the Spanish Project MTM2016-76969P from the Ministry of Economy and Competitiveness (MINECO/AEI/FEDER, UE), Spain.

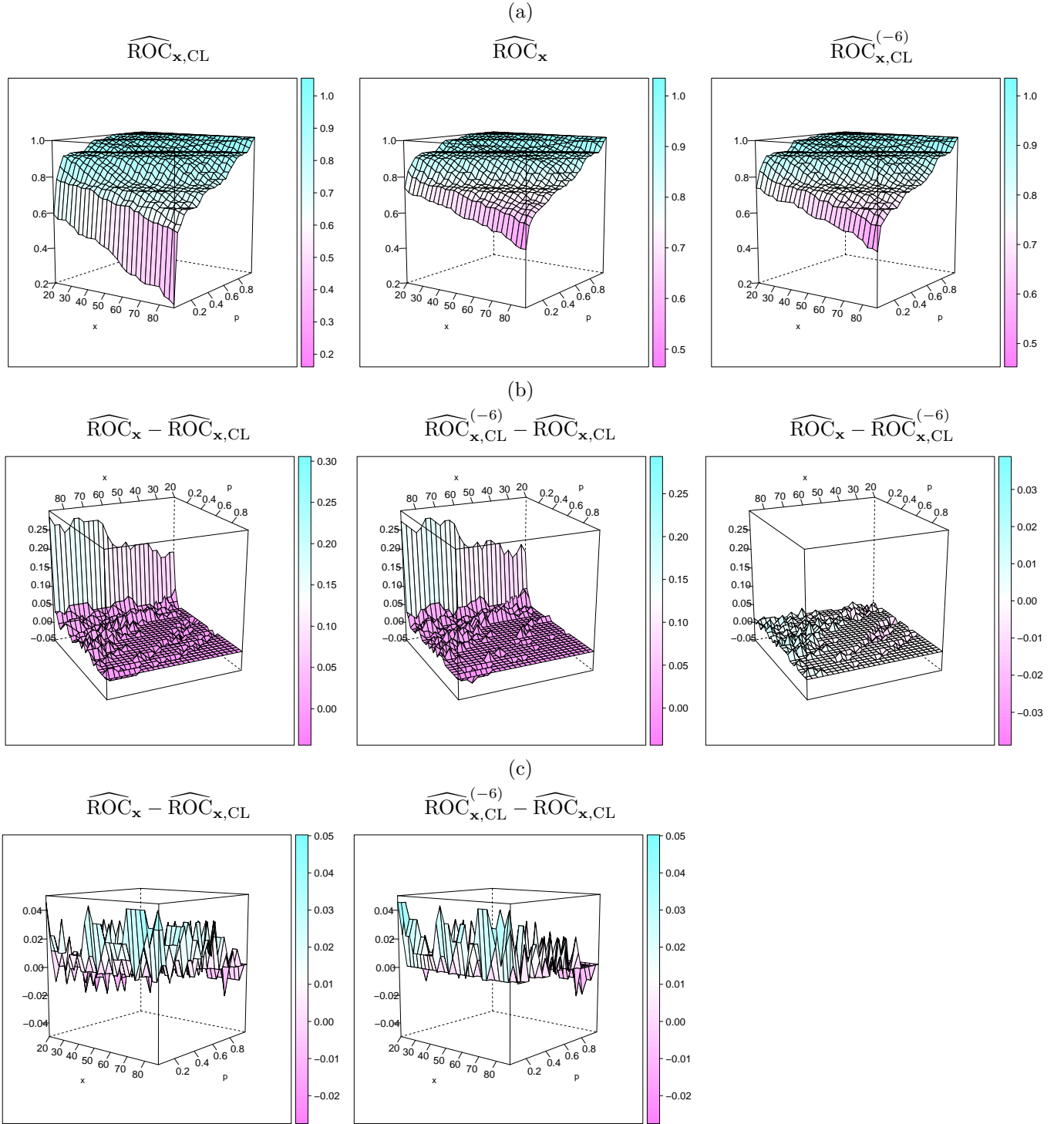


Figure 17: Diabetes Data: (a) Estimated ROC surfaces and (b) Difference between the estimated ROC surfaces (c) Difference between the estimated ROC surfaces between 0.045 and 0.99.

A Appendix A: Proof of Theorem 1.

We begin by proving (i). Using assumption **A3** for $j = H$ and the continuity of the quantile functionals when **A1** holds, we get that, for the healthy subjects, $\widehat{G}_H^{-1}(p) \xrightarrow{a.s.} G_H^{-1}(p)$, for each $0 < p < 1$. To avoid burden notation denote as

$$\begin{aligned}\widehat{\Delta}(\mathbf{x}, p) &= \frac{\widehat{\mu}_H(\mathbf{x}) - \widehat{\mu}_D(\mathbf{x})}{\widehat{\sigma}_D} + \frac{\widehat{\sigma}_H}{\widehat{\sigma}_D} \widehat{G}_H^{-1}(1 - p), \\ \Delta(\mathbf{x}, p) &= \frac{\mu_{0,H}(\mathbf{x}) - \mu_{0,D}(\mathbf{x})}{\sigma_{0,D}} + \frac{\sigma_{0,H}}{\sigma_{0,D}} G_H^{-1}(1 - p).\end{aligned}$$

Note that the consistency of $\widehat{\sigma}_j$ and **A4** together with the fact that $\widehat{G}_H^{-1}(p) \xrightarrow{a.s.} G_H^{-1}(p)$, entail that for each fixed p and \mathbf{x} , $\widehat{\Delta}(\mathbf{x}, p) \xrightarrow{a.s.} \Delta(\mathbf{x}, p)$. Therefore, we have that,

$$\begin{aligned}|\widehat{\text{ROC}}_{\mathbf{x}}(p) - \text{ROC}_{\mathbf{x}}(p)| &= \left| \widehat{G}_D \left(\widehat{\Delta}(\mathbf{x}, p) \right) - G_D \left(\Delta(\mathbf{x}, p) \right) \right| \\ &\leq \left| \widehat{G}_D \left(\widehat{\Delta}(\mathbf{x}, p) \right) - G_D \left(\widehat{\Delta}(\mathbf{x}, p) \right) \right| + \left| G_D \left(\widehat{\Delta}(\mathbf{x}, p) \right) - G_D \left(\Delta(\mathbf{x}, p) \right) \right| \\ &\leq \left\| \widehat{G}_D - G_D \right\|_{\infty} + \left| G_D \left(\widehat{\Delta}(\mathbf{x}, p) \right) - G_D \left(\Delta(\mathbf{x}, p) \right) \right|\end{aligned}$$

which together with the continuity of G_D lead to $\widehat{\text{ROC}}_{\mathbf{x}}(p) \xrightarrow{a.s.} \text{ROC}_{\mathbf{x}}(p)$, for each fixed \mathbf{x} and $0 < p < 1$. Note that for each fixed \mathbf{x} , $\text{ROC}_{\mathbf{x}}(p)$ satisfies the conditions in Lemma S.1.1, so $\sup_{0 < p < 1} |\widehat{\text{ROC}}_{\mathbf{x}}(p) - \text{ROC}_{\mathbf{x}}(p)| \xrightarrow{a.s.} 0$.

(ii) Using that

$$\begin{aligned}\left| \widehat{\Delta}(\mathbf{x}, p) - \Delta(\mathbf{x}, p) \right| &\leq \frac{1}{\widehat{\sigma}_D} \{ |\widehat{\mu}_H(\mathbf{x}) - \mu_{0,H}(\mathbf{x})| + |\widehat{\mu}_D(\mathbf{x}) - \mu_{0,D}(\mathbf{x})| \} \\ &\quad + \left| \frac{1}{\widehat{\sigma}_D} - \frac{1}{\sigma_{0,D}} \right| |\mu_{0,H}(\mathbf{x}) - \mu_{0,D}(\mathbf{x})| \\ &\quad + \frac{\widehat{\sigma}_H}{\widehat{\sigma}_D} \left| \widehat{G}_H^{-1}(1 - p) - G_H^{-1}(1 - p) \right| + |G_H^{-1}(1 - p)| \left| \frac{\widehat{\sigma}_H}{\widehat{\sigma}_D} - \frac{\sigma_{0,H}}{\sigma_{0,D}} \right|,\end{aligned}$$

assumption **A6**, the consistency of $\widehat{\sigma}_j$ and the uniform consistency of $\widehat{\mu}_j$, we get easily that $\sup_{\mathbf{x} \in \mathcal{K}} \left| \widehat{\Delta}(\mathbf{x}, p) - \Delta(\mathbf{x}, p) \right| \xrightarrow{a.s.} 0$. Hence,

$$\sup_{\mathbf{x} \in \mathcal{K}} |\widehat{\text{ROC}}_{\mathbf{x}}(p) - \text{ROC}_{\mathbf{x}}(p)| \leq \left\| \widehat{G}_D - G_D \right\|_{\infty} + \|g_D\|_{\infty} \sup_{\mathbf{x} \in \mathcal{K}} \left| \widehat{\Delta}(\mathbf{x}, p) - \Delta(\mathbf{x}, p) \right|$$

leads to $\sup_{\mathbf{x} \in \mathcal{K}} |\widehat{\text{ROC}}_{\mathbf{x}}(p) - \text{ROC}_{\mathbf{x}}(p)| \xrightarrow{a.s.} 0$.

Denote as $\widehat{B} = \sup_{\delta < p < 1-\delta} \sup_{\mathbf{x} \in \mathcal{K}} |\widehat{\text{ROC}}_{\mathbf{x}}(p) - \text{ROC}_{\mathbf{x}}(p)|$, then $\widehat{B} \leq \sum_{\ell=1}^5 \widehat{B}_{\ell}$ where

$$\begin{aligned}\widehat{B}_1 &= \left\| \widehat{G}_D - G_D \right\|_{\infty}, \\ \widehat{B}_2 &= \|g_D\|_{\infty} \left| \frac{1}{\widehat{\sigma}_D} - \frac{1}{\sigma_{0,D}} \right| (A_H + A_D), \\ \widehat{B}_3 &= \|g_D\|_{\infty} \frac{1}{\widehat{\sigma}_D} \sup_{\mathbf{x} \in \mathcal{K}} \{ |\widehat{\mu}_H(\mathbf{x}) - \mu_{0,H}(\mathbf{x})| + |\widehat{\mu}_D(\mathbf{x}) - \mu_{0,D}(\mathbf{x})| \}, \\ \widehat{B}_4 &= \frac{\widehat{\sigma}_H}{\widehat{\sigma}_D} \sup_{\delta < p < 1-\delta} \left| \widehat{G}_H^{-1}(1-p) - G_H^{-1}(1-p) \right|, \\ \widehat{B}_5 &= \sup_{\delta < p < 1-\delta} |G_H^{-1}(1-p)| \left| \frac{\widehat{\sigma}_H}{\widehat{\sigma}_D} - \frac{\sigma_{0,H}}{\sigma_{0,D}} \right|.\end{aligned}$$

Assumptions **A1** to **A3** together with **A5** and the consistency of $\widehat{\sigma}_j$ entail that $\widehat{B}_{\ell} \xrightarrow{a.s.} 0$, for $\ell = 1, 2, 3, 5$. Besides, using that $u = \widehat{G}_H^{-1}(\widehat{G}_H(u))$ and making the change $\widehat{G}_H(u) = 1-p$, we get that

$$\begin{aligned}\sup_{\delta < p < 1-\delta} \left| \widehat{G}_H^{-1}(1-p) - G_H^{-1}(1-p) \right| &= \sup_{\widehat{G}_H^{-1}(\delta) < u < \widehat{G}_H^{-1}(1-\delta)} \left| G_H^{-1}(\widehat{G}_H(u)) - u \right| \\ &\leq \sup_{\widehat{G}_H^{-1}(\delta) < u < \widehat{G}_H^{-1}(1-\delta)} \frac{1}{g_H(G_H^{-1}(\xi_u))} \left| \widehat{G}_H(u) - G_H(u) \right|\end{aligned}$$

where ξ_u is an intermediate point between $\widehat{G}_H(u)$ and $G_H(u)$. Using that $\widehat{G}_H^{-1}(1-\delta) \xrightarrow{a.s.} G_H^{-1}(1-\delta)$ and $\widehat{G}_H^{-1}(\delta) \xrightarrow{a.s.} G_H^{-1}(\delta)$ and that $G_H^{-1}(\delta/2) < G_H^{-1}(\delta)$ and $G_H^{-1}(1-\delta) < G_H^{-1}(1-\delta/2)$, since G_H has a density, we obtain that for all $\omega \notin \mathcal{N}$ with $\mathbb{P}(\mathcal{N}) = 1$, there exists $N_{0,H}$ such that for $n_H \geq N_{0,H}$, $a(\delta) = G_H^{-1}(\delta/2) < \widehat{G}_H^{-1}(\delta)$ and $\widehat{G}_H^{-1}(1-\delta) < G_H^{-1}(1-\delta/2) = b(\delta)$. Thus, $\xi_u \in [a(\delta), b(\delta)] = \mathcal{I}$ so using that $i(\delta) = \inf_{u \in \mathcal{I}} g_H(u) > 0$, we conclude that

$$\sup_{\delta < p < 1-\delta} \left| \widehat{G}_H^{-1}(1-p) - G_H^{-1}(1-p) \right| \leq i(\delta) \sup_{a(\delta) < u < b(\delta)} \left| \widehat{G}_H(u) - G_H(u) \right| \leq i(\delta) \|\widehat{G}_H - G_H\|_{\infty},$$

concluding the proof of (ii).

We now proceed to derive (iii). Let $\epsilon > 0$ be fixed and choose $0 < \eta < 1$ such that,

$\sup_{\mathbf{x} \in \mathcal{K}} \text{ROC}_{\mathbf{x}}(\eta) < \epsilon/6$ and $\sup_{\mathbf{x} \in \mathcal{K}} (1 - \text{ROC}_{\mathbf{x}}(1 - \eta)) < \epsilon/6$. Denote as

$$\begin{aligned}\widehat{B}(\eta) &= \sup_{\eta < p < 1-\eta} \sup_{\mathbf{x} \in \mathcal{K}} |\widehat{\text{ROC}}_{\mathbf{x}}(p) - \text{ROC}_{\mathbf{x}}(p)|, \\ \widehat{B}_1(\eta) &= \sup_{p \leq \eta} \sup_{\mathbf{x} \in \mathcal{K}} |\widehat{\text{ROC}}_{\mathbf{x}}(p) - \text{ROC}_{\mathbf{x}}(p)|, \\ \widehat{B}_2(\eta) &= \sup_{1-\eta \leq p} \sup_{\mathbf{x} \in \mathcal{K}} |\widehat{\text{ROC}}_{\mathbf{x}}(p) - \text{ROC}_{\mathbf{x}}(p)|.\end{aligned}$$

Hence, $\sup_{0 < p < 1} \sup_{\mathbf{x} \in \mathcal{K}} |\widehat{\text{ROC}}_{\mathbf{x}}(p) - \text{ROC}_{\mathbf{x}}(p)| \leq \widehat{B}(\eta) + \widehat{B}_1(\eta) + \widehat{B}_2(\eta)$. From (ii), $\widehat{B}(\eta) \xrightarrow{a.s.} 0$. Besides, using that $\text{ROC}_{\mathbf{x}}(p)$ is a distribution function and $\widehat{\text{ROC}}_{\mathbf{x}}(p)$ is non-decreasing in p , we get that for any $p \leq \eta$, $\mathbf{x} \in \mathcal{K}$,

$$|\widehat{\text{ROC}}_{\mathbf{x}}(p) - \text{ROC}_{\mathbf{x}}(p)| \leq \max \left\{ \widehat{\text{ROC}}_{\mathbf{x}}(\eta), \text{ROC}_{\mathbf{x}}(\eta) \right\},$$

so $\widehat{B}_1(\eta) \leq \sup_{\mathbf{x} \in \mathcal{K}} \max \left\{ \widehat{\text{ROC}}_{\mathbf{x}}(\eta), \text{ROC}_{\mathbf{x}}(\eta) \right\} = \widehat{C}_1(\eta)$. Similarly, we obtain that $\widehat{B}_2(\eta) \leq \sup_{\mathbf{x} \in \mathcal{K}} \max \left\{ 1 - \widehat{\text{ROC}}_{\mathbf{x}}(1 - \eta), 1 - \text{ROC}_{\mathbf{x}}(1 - \eta) \right\} = \widehat{C}_2(\eta)$.

Using that $\sup_{\mathbf{x} \in \mathcal{K}} \text{ROC}_{\mathbf{x}}(\eta) < \epsilon$ and $\sup_{\mathbf{x} \in \mathcal{K}} (1 - \text{ROC}_{\mathbf{x}}(1 - \eta)) < \epsilon$ and that for any fixed $0 < p < 1$, $\sup_{\mathbf{x} \in \mathcal{K}} |\widehat{\text{ROC}}_{\mathbf{x}}(p) - \text{ROC}_{\mathbf{x}}(p)| \xrightarrow{a.s.} 0$, we conclude that there exists \mathcal{N} such that $\mathbb{P}(\mathcal{N}) = 0$ and for $\omega \notin \mathcal{N}$, $\widehat{B}(\eta) \rightarrow 0$, $\widehat{C}_1(\eta) \rightarrow \sup_{\mathbf{x} \in \mathcal{K}} \text{ROC}_{\mathbf{x}}(\eta) < \epsilon/6$ and $\widehat{C}_2(\eta) \rightarrow \sup_{\mathbf{x} \in \mathcal{K}} 1 - \text{ROC}_{\mathbf{x}}(1 - \eta) < \epsilon/6$. Hence, for n_H and n_D large enough, we obtain that $\widehat{B}(\eta) < \epsilon/3$, $\widehat{C}_\ell(\eta) < \epsilon/3$, for $\ell = 1, 2$ which leads to $\sup_{0 < p < 1} \sup_{\mathbf{x} \in \mathcal{K}} |\widehat{\text{ROC}}_{\mathbf{x}}(p) - \text{ROC}_{\mathbf{x}}(p)| \leq \epsilon$, concluding the proof. \blacksquare

B Appendix B

In this section, we investigate the validity of assumption **A3**. For that purpose, we will derive the uniform strong consistency of $\widehat{G}_n(t)$ defined in (6) in two situations, under a linear model or a non-linear one, since for the former we can also include a hard rejection weight function to define the weights w_i . It is worth noticing that our results generalize those given in Gervini and Yohai (2002) in two directions: we extend their results beyond

the linear model to a non-linear one and we obtain almost surely uniform consistency instead of results in probability.

From now on, for any measure Q , we denote as $N(\epsilon, \mathcal{F}, L_s(Q))$ and $N_{[\cdot]}(\epsilon, \mathcal{F}, L_s(Q))$ the covering and bracketing numbers of the class \mathcal{F} with respect to the distance in $L_s(Q)$, as defined, for instance, in van der Vaart and Wellner (1996).

B.1 Linear Model

Throughout this section, we will assume that we have a random sample $(y_1, \mathbf{x}_1), \dots, (y_n, \mathbf{x}_n)$, where \mathbf{x}_i is a vector of p explanatory variables and y_i is a response variable that satisfy the linear regression model

$$y_i = \mathbf{x}_i^T \boldsymbol{\beta}_0 + u_i = \mathbf{x}_i^T \boldsymbol{\beta}_0 + \sigma_0 \epsilon_i, i = 1 \dots n,$$

with $\boldsymbol{\beta}_0 \in \mathbb{R}^p$ and the errors ϵ_i are i.i.d. and independent of \mathbf{x}_i with unknown distribution $G_0(\cdot)$ and σ_0 is the scale parameter. As above, we will assume that G_0 is symmetric around 0.

From now on, $\hat{\boldsymbol{\beta}}$ and $\hat{\sigma}$ stand for robust consistent estimators of $\boldsymbol{\beta}_0$ and σ_0 , so the standardized residuals are given by

$$r_i = \frac{y_i - \mathbf{x}_i^T \hat{\boldsymbol{\beta}}}{\hat{\sigma}}.$$

Based on the residuals the adaptive weighted empirical distribution given in (6) is defined using the weights $w_i = w(r_i/t_n)$ defined in (8) with t_n given in (7).

To derive uniform consistency results, we will need the following set of assumptions:

- C1** The weight function $w : \mathbb{R} \rightarrow [0, 1]$ is even, non-increasing on $[0, +\infty)$, continuous, $w(0) = 1$, $w(u) > 0$ for $0 < u < 1$ and $w(u) = 0$ for $|u| \geq 1$.
- C2** G_0 is a continuous distribution function, symmetric around 0.

C3 The estimators $\widehat{\beta}$ and $\widehat{\sigma}$ are such that $\widehat{\beta} \xrightarrow{a.s.} \beta_0$ and $\widehat{\sigma} \xrightarrow{a.s.} \sigma_0$.

Define the values

$$\begin{aligned} d_0 &= \sup_{t \geq 0} \{G^+(t) - G_0^+(t)\}^+ = \sup_{t \geq 0} \{\max(G^+(t) - G_0^+(t), 0)\} \\ \bar{t}_0 &= (G_0^+)^{-1}(1 - d_0) = G_0^{-1}\left(1 - \frac{d_0}{2}\right) \\ t_0 &= \max(\bar{t}_0, \eta) \end{aligned}$$

As mentioned in Gervini and Yohai (2002), when G^+ is stochastically larger or equal than G_0^+ , we have that $t_0 = \infty$, so \widehat{G}_n defined in (6) will converge to G_0 . Furthermore, consider the functions

$$h_\infty(t) = \mathbb{E}_{G_0} w\left(\frac{\epsilon_1}{t}\right) \quad (\text{B.1})$$

$$h_0(t, s) = \mathbb{E}_{G_0} w\left(\frac{\epsilon_1}{t}\right) \mathbb{I}_{\epsilon_1 \leq s} \quad (\text{B.2})$$

The following lemma is a well known result regarding continuous distributions, whose proof we include for completeness.

Lemma 1. *Let $F_n : \mathbb{R} \rightarrow [0, 1]$ and $F : \mathbb{R} \rightarrow [0, 1]$ be non-decreasing functions such that F is continuous, $\lim_{t \rightarrow +\infty} F(t) = 1$ and $\lim_{t \rightarrow -\infty} F(t) = 0$. Then, if $F_n(t) \xrightarrow{a.s.} F(t)$, for any $t \in \mathbb{R}$, we also have that $\|F_n - F\|_\infty \xrightarrow{a.s.} 0$.*

PROOF. Given $\epsilon > 0$, let a and b be such that $F(a) < \epsilon$ and $F(b) > 1 - \epsilon$. Furthermore, using that F is uniformly continuous on $[a, b]$, we get that there exists δ such that

$$|t - s| < \delta, t, s \in [a, b] \Rightarrow |F(t) - F(s)| < \epsilon$$

Let $a = a_0 < a_2 < \dots < a_k = b$, be a grid such that $a_j - a_{j-1} < \delta$, $1 \leq j \leq k$. Then, we have that for any $t < a$, $F_n(t) - F(t) \leq F_n(a) \leq F_n(a) - F(a) + F(a) \leq |F_n(a) - F(a)| + \epsilon$, while $F(t) - F_n(t) \leq F(a) < \epsilon$, so

$$\sup_{t < a} |F_n(t) - F(t)| \leq |F_n(a) - F(a)| + \epsilon. \quad (\text{B.3})$$

Similarly,

$$\sup_{t > b} |F_n(t) - F(t)| \leq |F_n(b) - F(b)| + \epsilon. \quad (\text{B.4})$$

Finally, given $t \in [a, b]$, there exists $1 \leq j \leq k$ such that $t \in [a_{j-1}, a_j]$, so that

$$\begin{aligned} F_n(t) - F(t) &\leq F_n(a_j) - F(a_{j-1}) \leq F_n(a_j) - F(a_j) + F(a_j) - F(a_{j-1}) \\ &\leq \epsilon + \max_{1 \leq j \leq k} |F_n(a_j) - F(a_j)|. \end{aligned}$$

Similarly,

$$\begin{aligned} F(t) - F_n(t) &\leq F(a_j) - F_n(a_{j-1}) \leq F(a_j) - F(a_{j-1}) + F(a_{j-1}) - F_n(a_{j-1}) \\ &\leq \epsilon + \max_{1 \leq j \leq k} |F_n(a_j) - F(a_j)|, \end{aligned}$$

so

$$\sup_{a \leq t \leq b} |F_n(t) - F(t)| \leq \epsilon + \max_{1 \leq j \leq k} |F_n(a_j) - F(a_j)|. \quad (\text{B.5})$$

Let \mathcal{N} be such that, for $\omega \notin \mathcal{N}$, $F_n(a_j) \rightarrow F(a_j)$ and $\mathbb{P}(\mathcal{N}) = 0$. Then, using (B.3), (B.4) and (B.5) we get that

$$\mathbb{P}(\limsup \|F_n - F\|_\infty < \epsilon) = 1,$$

for any $\epsilon > 0$, concluding the proof. ■

Lemma 2. *Under **C2** and **C3**, we have that*

$$a) \ \|G_n^+ - G_0^+\|_\infty \xrightarrow{a.s.} 0.$$

$$b) \ d_n \xrightarrow{a.s.} d_0.$$

$$c) \ \bar{t}_n \xrightarrow{a.s.} \bar{t}_0.$$

PROOF. a) Let us consider the family of functions

$$\mathcal{F} = \{f_{\boldsymbol{\theta}, \kappa}(u, \mathbf{x}) = \mathbb{I}_{|u - \mathbf{x}^T \boldsymbol{\theta}| \leq \kappa t} \text{ for } (\boldsymbol{\theta}, t, \kappa) \in \mathbb{R}^p \times \mathbb{R}_{\geq 0} \times \mathbb{R}_{> 0}\}.$$

First, note that

$$f_{\boldsymbol{\theta}, \kappa}(u, \mathbf{x}) = \mathbb{I}_{|u - \mathbf{x}^T \boldsymbol{\theta}| \leq \kappa t} = \mathbb{I}_{C_{(\kappa^{-1}, \boldsymbol{\theta} \kappa^{-1}, t)}},$$

where the set $C_{(s, \boldsymbol{\theta}, t)} = A_{(s, \boldsymbol{\theta}, t)} \cap B_{(s, \boldsymbol{\theta}, t)}$, with $A_{(s, \boldsymbol{\theta}, t)} = \{(u, \mathbf{x}) \in \mathbb{R}^{p+1} : su - \mathbf{x}^T \boldsymbol{\theta} - t \leq 0\}$ and $B_{(s, \boldsymbol{\theta}, t)} = \{(u, \mathbf{x}) \in \mathbb{R}^{p+1} : 0 \leq su - \mathbf{x}^T \boldsymbol{\theta} + t\}$. Define the classes of sets

$$\begin{aligned}\mathcal{A} &= \{A_{(s, \boldsymbol{\theta}, t)} : (\boldsymbol{\theta}, s, t) \in \mathbb{R}^p \times \mathbb{R}_{\geq 0} \times \mathbb{R}_{> 0}\} \\ \mathcal{B} &= \{B_{(s, \boldsymbol{\theta}, t)} : (\boldsymbol{\theta}, s, t) \in \mathbb{R}^p \times \mathbb{R}_{\geq 0} \times \mathbb{R}_{> 0}\}.\end{aligned}$$

Taking into account that $\{g(u, \mathbf{x}) = su - \mathbf{x}^T \boldsymbol{\theta} - t; (\boldsymbol{\theta}, s, t) \in \mathbb{R}^p \times \mathbb{R}_{\geq 0} \times \mathbb{R}_{> 0}\}$ is a finite-dimensional space of functions with dimension $p + 2$, from Lemmas 9.6, 9.8 and 9.9 in Kosorok (2008) we get that \mathcal{A} and \mathcal{B} are VC-classes with index at most $p + 4$. Furthermore, $\mathcal{C} = \mathcal{A} \cap \mathcal{B}$ is also a VC-class with index smaller or equal than $2p + 7$. Taking into account that $C_{(s, \boldsymbol{\theta})} \in \mathcal{C}$, applying again Lemma 9.8 in Kosorok (2008), we get that the class of functions \mathcal{F} is a VC-class with index $V(\mathcal{F})$ smaller or equal than $2p + 7$. Note that the envelope of \mathcal{F} equals $F \equiv 1$. Hence, Theorem 2.6.7 in van der Vaart and Wellner (1996) entails that, there exists a universal constant K such that, for any measure Q

$$N(\epsilon, \mathcal{F}, L_1(Q)) \leq K V(\mathcal{F}) (16e)^{V(\mathcal{F})} \left(\frac{1}{\epsilon}\right)^{V(\mathcal{F})-1},$$

which together with Theorem 2.4.3 in van der Vaart and Wellner (1996) or Theorem 2.4 in Kosorok (2008), leads to

$$\sup_{f \in \mathcal{F}} |P_n f - P f| \xrightarrow{a.s.} 0, \quad (\text{B.6})$$

where we have used the standard notation in empirical processes, i.e., $P f = \mathbb{E} f(u, \mathbf{x})$ and $P_n f = (1/n) \sum_{i=1}^n f(u_i, \mathbf{x}_i)$.

Note that G_n^+ can be written as

$$G_n^+(t) = P_n f_{\hat{\boldsymbol{\theta}}, \hat{\sigma}_t}(u_i, \mathbf{x}_i)$$

with $\hat{\boldsymbol{\theta}} = \hat{\boldsymbol{\beta}} - \boldsymbol{\beta}_0$. Denote as $M(\boldsymbol{\theta}, \kappa) = P f_{\boldsymbol{\theta}, \kappa}(u, \mathbf{x})$. Then, using (B.6), we conclude that

$$\sup_{t \geq 0} |G_n^+(t) - M(\hat{\boldsymbol{\theta}}, \hat{\sigma}_t)| \leq \sup_{f \in \mathcal{F}} |P_n f - P f| \xrightarrow{a.s.} 0.$$

It remains to show that

$$\sup_{t \geq 0} \left| M(\widehat{\boldsymbol{\theta}}, \widehat{\sigma} t) - G_0^+(t) \right| \xrightarrow{a.s.} 0.$$

Note that

$$M(\boldsymbol{\theta}, \kappa) = Pf_{\boldsymbol{\theta}, \kappa}(u, \mathbf{x}) = \mathbb{P}(|u - \mathbf{x}^T \boldsymbol{\theta}| \leq \kappa),$$

hence

$$M(0, \sigma_0 t) = \mathbb{P}(|u| \leq \sigma_0 t) = G_0^+(t).$$

Therefore, we have to show that

$$\sup_{t \geq 0} \left| M(\widehat{\boldsymbol{\theta}}, \widehat{\sigma} t) - M(0, \sigma_0 t) \right| \xrightarrow{a.s.} 0.$$

First observe that

$$\begin{aligned} M(\boldsymbol{\theta}, \kappa) &= \mathbb{P}(-\kappa + \mathbf{x}^T \boldsymbol{\theta} \leq u \leq \kappa + \mathbf{x}^T \boldsymbol{\theta}) \\ &= \mathbb{E} \left\{ G_0(\mathbf{x}^T \boldsymbol{\theta} + \kappa) - G_0(\mathbf{x}^T \boldsymbol{\theta} - \kappa) \right\}. \end{aligned}$$

The continuity of G_0 and the Dominated Convergence Theorem entail that $M(\boldsymbol{\theta}, \kappa)$ is a continuous function of its arguments, which together with **C3**, entails that $M(\widehat{\boldsymbol{\theta}}, \widehat{\sigma} t) - M(0, \sigma_0 t) \xrightarrow{a.s.} 0$, for each fixed t . Now

$$\widehat{M}(t) = M(\widehat{\boldsymbol{\theta}}, \widehat{\sigma} t) = \mathbb{P} \left(\frac{|u - \mathbf{x}^T \widehat{\boldsymbol{\theta}}|}{\widehat{\sigma}} \leq t \right)$$

is a bounded monotone function of t , while $M(0, \sigma_0 t) = G_0^+(t)$ is also bounded, monotone and continuous, thus, from Lemma 1 we obtain that the convergence is indeed uniform, that is, $\sup_{t \geq 0} \left| M(\widehat{\boldsymbol{\theta}}, \widehat{\sigma} t) - M(0, \sigma_0 t) \right| \xrightarrow{a.s.} 0$, concluding the proof of a).

b) As in Gervini and Yohai (2002), $|d_n - d_0| \leq \|G_n^+ - G_0^+\|_\infty$ and the result follows.

c) To show that $\bar{t}_n \xrightarrow{a.s.} \bar{t}_0$, it is enough to show that $G_0^+(\bar{t}_n) \xrightarrow{a.s.} G_0^+(\bar{t}_0) = 1 - d_0$ which follows from Lemma 3.1 in Gervini and Yohai (2002) distinguishing the cases $\bar{t}_0 < \infty$ and $\bar{t}_0 = \infty$. ■

Lemma 3. Assume that either $w(t) = \mathbb{I}_{[-1,1]}(t)$ or w satisfies **C1**. Then, we have that $\sup_{f \in \mathcal{F}} |P_n f - P f| \xrightarrow{a.s.} 0$, where

$$\mathcal{F} = \{f_{\boldsymbol{\theta}, \kappa, \nu}(u, \mathbf{x}) = w(\nu(u - \mathbf{x}^T \boldsymbol{\theta})) \mathbb{I}_{u - \mathbf{x}^T \boldsymbol{\theta} \leq \kappa s} \text{ for } (\boldsymbol{\theta}, \kappa, \nu) \in \mathbb{R}^p \times \mathbb{R}_{\geq 0} \times \mathbb{R}_{\geq 0}\}.$$

PROOF. Assume that w satisfies **C1** and note that $\mathcal{F} \subset \mathcal{F}_1 \cdot \mathcal{F}_2$ where

$$\mathcal{F}_1 = \{f_{\boldsymbol{\theta}, \nu}(u, \mathbf{x}) = w(\nu(u - \mathbf{x}^T \boldsymbol{\theta})) \text{ for } (\boldsymbol{\theta}, \nu) \in \mathbb{R}^p \times \mathbb{R}_{\geq 0}\}$$

$$\mathcal{F}_2 = \{f_{\boldsymbol{\theta}, \kappa}(u, \mathbf{x}) = \mathbb{I}_{u - \mathbf{x}^T \boldsymbol{\theta} \leq \kappa s} \text{ for } (\boldsymbol{\theta}, \kappa) \in \mathbb{R}^p \times \mathbb{R}_{\geq 0}\}.$$

The classes \mathcal{F} , \mathcal{F}_1 and \mathcal{F}_2 have envelope 1, hence we have easily that, for any measure Q ,

$$N(2\epsilon, \mathcal{F}, L_1(Q)) \leq N(\epsilon, \mathcal{F}_1, L_1(Q)) N(\epsilon, \mathcal{F}_2, L_1(Q)),$$

so that to show $\sup_{f \in \mathcal{F}} |P_n f - P f| \xrightarrow{a.s.} 0$, it will be enough to prove that, for $j = 1, 2$,

$$\frac{1}{n} \log N(\epsilon, \mathcal{F}_j, L_1(P_n)) \xrightarrow{p} 0. \quad (\text{B.7})$$

As in the proof of Lemma 2, it is easy to see that \mathcal{F}_2 is a VC-class with index $V_2 = p + 3$, so

$$N(\epsilon, \mathcal{F}_2, L_1(Q)) \leq K V_2 (16e)^{V_2} \left(\frac{1}{\epsilon}\right)^{V_2-1},$$

leading to (B.7), when $j = 2$.

On the other hand, the family

$$\mathcal{R} = \{\nu(u - \mathbf{x}^T \boldsymbol{\theta}) : \boldsymbol{\theta} \in \mathbb{R}^p, \nu \in \mathbb{R}_{\geq 0}\}$$

is a subset of the vector space of all linear functions in $p + 1$ variables. It follows from Lemma 2.6.15 of van der Vaart and Wellner (1996) that \mathcal{R} has VC-index at most $p + 3$. Note that w is an even function, non-increasing on $[0, +\infty)$, hence it can be written as $w = w^{(1)} + w^{(2)}$, where $w^{(1)}(x) = w(x) \mathbb{I}_{[0, +\infty)}(x)$ is non-increasing and $w^{(2)}(x) = w(x) \mathbb{I}_{(-\infty, 0)}(x)$ is non-decreasing. Using the permanence property for VC-classes, see Lemma 9.9 in Kosorok (2008), we obtain that the classes of functions $\mathcal{R}_{w^{(1)}} = w^{(1)} \circ \mathcal{R}$

and $\mathcal{R}_{w^{(2)}} = w^{(2)} \circ \mathcal{R}$ are VC-classes with VC-index at most $p+3$. Furthermore, the classes $\mathcal{R}_{w^{(j)}}$, $j = 1, 2$, have envelope 1. Then, Theorem 2.6.7 of Van der Vaart and Wellner (1996) implies that there exists a universal constant K such that, for any probability measure Q on \mathbb{R}^{p+1} and any $0 < \epsilon < 1$, we have that

$$N(\epsilon, \mathcal{R}_{w^{(j)}}, L_1(Q)) \leq K(p+3) (16e)^{(p+3)} \left(\frac{1}{\epsilon}\right)^{p+2}.$$

Note that $\mathcal{R}_{w^{(1)}} + \mathcal{R}_{w^{(2)}}$ has also constant envelope equal to 2. Therefore,

$$\begin{aligned} N(2\epsilon, \mathcal{R}_{w^{(1)}} + \mathcal{R}_{w^{(2)}}, L_1(Q)) &\leq N(\epsilon, \mathcal{R}_{w^{(1)}}, L_1(Q)) \times N(\epsilon, \mathcal{R}_{w^{(2)}}, L_1(Q)) \\ &\leq \left[K(p+3) (16e)^{(p+3)} \left(\frac{1}{\epsilon}\right)^{p+2} \right]^2. \end{aligned}$$

Finally noting that \mathcal{F}_1 has constant envelope equal to 1 and $\mathcal{F}_1 \subset \mathcal{R}_{w^{(1)}} + \mathcal{R}_{w^{(2)}}$, we get that

$$N(2\epsilon, \mathcal{F}_1, L_1(P_n)) \leq \left[K(p+3) (16e)^{(p+3)} \left(\frac{1}{\epsilon}\right)^{p+2} \right]^2,$$

concluding the proof.

When $w(t) = \mathbb{I}_{[-1,1]}(t)$ the result is straightforward using that

$$\mathcal{F}_1 = \{f_{\boldsymbol{\theta}, \nu}(u, \mathbf{x}) = \mathbb{I}_{\nu(u - \mathbf{x}^T \boldsymbol{\theta}) \leq 1} \mathbb{I}_{-\nu(u - \mathbf{x}^T \boldsymbol{\theta}) \leq 1} \text{ for } (\boldsymbol{\theta}, \nu) \in \mathbb{R}^p \times \mathbb{R}_{\geq 0}\}$$

and similar arguments to those consider above. ■

Proposition 1. *Assume that $w(t) = \mathbb{I}_{[-1,1]}(t)$ or w satisfies **C1**. Under **C2** to **C3**, we have that*

a) if $t_0 < \infty$,

$$\sup_{s \in \mathbb{R}} \left| \widehat{G}_n(s) - \frac{h_0(t_0, s)}{h_\infty(t_0)} \right| \xrightarrow{a.s.} 0,$$

with $h_\infty(t_0)$ and $h_0(t_0, s)$ defined in (B.1) and (B.2), respectively.

b) if $t_0 = \infty$, $\|\widehat{G}_n - G_0\|_\infty \xrightarrow{a.s.} 0$.

PROOF. When $t_0 = \infty$, using that G_0 is a bounded, monotone and continuous function and that \widehat{G}_n is monotone, it will be enough to show that for each $s \in \mathbb{R}$, $\widehat{G}_n(s) \xrightarrow{a.s.} G(s)$. On the other hand, when $t_0 < \infty$, standard arguments allow to show that $F(s) = h_1(t_0, s)/h_\infty(t_0)$ is a bounded, monotone and continuous function of s and the uniform convergence also follows from the pointwise one.

Denote as $\widehat{\nu}_n = 1/(t_n \widehat{\sigma}_n)$, $\nu_0 = 1/(t_0 \sigma_0)$, where we understand that if $t_0 = +\infty$, $\nu_0 = 0$. Then $\widehat{\nu}_n \xrightarrow{a.s.} \nu_0$.

We will begin by showing that

$$\frac{1}{n} \sum_{i=1}^n w_i I(r_i \leq s) \xrightarrow{a.s.} h_0(t_0, s) = \begin{cases} \mathbb{E}_{G_0} w \left(\frac{\epsilon_1}{t_0} \right) \mathbb{I}_{\epsilon_1 \leq s} & \text{if } t_0 < \infty \\ \mathbb{E}_{G_0} \mathbb{I}_{\epsilon_1 \leq s} = G_0(s) & \text{if } t_0 = \infty. \end{cases} \quad (\text{B.8})$$

For that purpose and noting that $r_i = (u_i - \mathbf{x}_i^T \widehat{\boldsymbol{\theta}})/\widehat{\sigma}$ with $\widehat{\boldsymbol{\theta}} = \widehat{\boldsymbol{\beta}} - \boldsymbol{\beta}_0$, define the class of functions

$$\mathcal{F} = \{f_{\boldsymbol{\theta}, \kappa, \nu}(u, \mathbf{x}) = w(\nu(u - \mathbf{x}^T \boldsymbol{\theta})) \mathbb{I}_{u - \mathbf{x}^T \boldsymbol{\theta} \leq \kappa s} \text{ for } (\boldsymbol{\theta}, \kappa, \nu) \in \mathbb{R}^p \times \mathbb{R}_{\geq 0} \times \mathbb{R}_{\geq 0}\}.$$

Lemma 3 entails that

$$\sup_{f \in \mathcal{F}} |P_n f - P f| \xrightarrow{a.s.} 0,$$

then, using that

$$\frac{1}{n} \sum_{i=1}^n w_i I(r_i \leq s) = P_n f_{\widehat{\boldsymbol{\theta}}, \widehat{\sigma}, \widehat{\nu}_n},$$

we obtain that

$$\frac{1}{n} \sum_{i=1}^n w_i I(r_i \leq s) - P f_{\widehat{\boldsymbol{\theta}}, \widehat{\sigma}, \widehat{\nu}_n} \xrightarrow{a.s.} 0.$$

It remains to show that

$$P f_{\widehat{\boldsymbol{\theta}}, \widehat{\sigma}, \widehat{\nu}_n} \xrightarrow{a.s.} P f_{0, \sigma_0, \nu_0} = h_0(t_0, s),$$

which will follow if we derive that

$$A_n = P f_{\widehat{\boldsymbol{\theta}}, \widehat{\sigma}, \widehat{\nu}_n} - \mathbb{E} w(\nu_0 u) \mathbb{I}_{u - \mathbf{x}^T \widehat{\boldsymbol{\theta}} \leq \widehat{\sigma} s} \xrightarrow{a.s.} 0 \quad (\text{B.9})$$

$$B_n = \mathbb{E} w(\nu_0 u) \mathbb{I}_{u - \mathbf{x}^T \widehat{\boldsymbol{\theta}} \leq \widehat{\sigma} s} - h_0(t_0, s) \xrightarrow{a.s.} 0. \quad (\text{B.10})$$

We begin by considering the situation where w satisfies **C1**. Noting that

$$\begin{aligned} |A_n| &= \left| \mathbb{E} \left\{ w \left(\nu_n(u - \mathbf{x}^T \hat{\boldsymbol{\theta}}) \right) - w(\nu_0 u) \right\} \mathbb{I}_{u - \mathbf{x}^T \hat{\boldsymbol{\theta}} \leq \hat{\sigma} s} \right| \\ &\leq \mathbb{E} \left| w \left(\nu_n(u - \mathbf{x}^T \hat{\boldsymbol{\theta}}) \right) - w(\nu_0 u) \right|, \end{aligned}$$

using the Dominated Convergence Theorem, the continuity of w and the fact that $\hat{\nu}_n \xrightarrow{a.s.} \nu_0$ and $\hat{\boldsymbol{\theta}} \xrightarrow{a.s.} 0$, we obtain that $A_n \xrightarrow{a.s.} 0$, concluding the proof of (B.9).

When $w = \mathbb{I}_{[-1,1]}$, we have that

$$\begin{aligned} w \left(\nu_n(u - \mathbf{x}^T \hat{\boldsymbol{\theta}}) \right) - w(\nu_0 u) &= \mathbb{I}_{\nu_n(u - \mathbf{x}^T \hat{\boldsymbol{\theta}}) \leq 1} \mathbb{I}_{-1 \leq \nu_n(u - \mathbf{x}^T \hat{\boldsymbol{\theta}})} - \mathbb{I}_{\nu_0 u \leq 1} \mathbb{I}_{-1 \leq \nu_0 u} \\ &= \mathbb{I}_{\nu_n(u - \mathbf{x}^T \hat{\boldsymbol{\theta}}) \leq 1} \left\{ \mathbb{I}_{-1 \leq \nu_n(u - \mathbf{x}^T \hat{\boldsymbol{\theta}})} - \mathbb{I}_{-1 \leq \nu_0 u} \right\} \\ &\quad + \left\{ \mathbb{I}_{\nu_0 u \leq 1} - \mathbb{I}_{\nu_n(u - \mathbf{x}^T \hat{\boldsymbol{\theta}}) \leq 1} \right\} \mathbb{I}_{-1 \leq \nu_0 u}, \end{aligned}$$

so

$$\begin{aligned} |A_n| &\leq \mathbb{E} \left| w \left(\nu_n(u - \mathbf{x}^T \hat{\boldsymbol{\theta}}) \right) - w(\nu_0 u) \right| \\ &\leq \mathbb{E} \left| \mathbb{I}_{-1 \leq \nu_n(u - \mathbf{x}^T \hat{\boldsymbol{\theta}})} - \mathbb{I}_{-1 \leq \nu_0 u} \right| + \mathbb{E} \left| \mathbb{I}_{\nu_0 u \leq 1} - \mathbb{I}_{\nu_n(u - \mathbf{x}^T \hat{\boldsymbol{\theta}}) \leq 1} \right| \\ &\leq \mathbb{E} \left| \mathbb{I}_{-\frac{1}{\nu_n} + \mathbf{x}^T \hat{\boldsymbol{\theta}} \leq u} - \mathbb{I}_{-\frac{1}{\nu_0} \leq u} \right| + \mathbb{E} \left| \mathbb{I}_{u \leq \frac{1}{\nu_0}} - \mathbb{I}_{u \leq \frac{1}{\nu_n} + \mathbf{x}^T \hat{\boldsymbol{\theta}}} \right| \\ &\leq \mathbb{E} \left| \mathbb{I}_{u < -\frac{1}{\nu_n} + \mathbf{x}^T \hat{\boldsymbol{\theta}}} - \mathbb{I}_{u < -\frac{1}{\nu_0}} \right| + \mathbb{E} \left| \mathbb{I}_{u \leq \frac{1}{\nu_0}} - \mathbb{I}_{u \leq \frac{1}{\nu_n} + \mathbf{x}^T \hat{\boldsymbol{\theta}}} \right| \\ &\leq \mathbb{E} \left| G_0 \left(\frac{1}{\sigma_0} \left[-\frac{1}{\nu_n} + \mathbf{x}^T \hat{\boldsymbol{\theta}} \right] \right) - G_0 \left(-\frac{1}{\sigma_0 \nu_0} \right) \right| + \mathbb{E} \left| G_0 \left(\frac{1}{\sigma_0} \left[\frac{1}{\nu_n} + \mathbf{x}^T \hat{\boldsymbol{\theta}} \right] \right) - G_0 \left(\frac{1}{\sigma_0 \nu_0} \right) \right|, \end{aligned}$$

where we understand that $\mathbb{I}_{u < -1/\nu_0} = 0$, $G_0(-1/\sigma_0 \nu_0) = 0$, $\mathbb{I}_{u < 1/\nu_0} = 1$ and $G_0(1/\sigma_0 \nu_0) = 1$ if $\nu_0 = 0$. Now the proof follows from the continuity of G_0 is $t_0 < \infty$ and from the fact that $\lim_{u \rightarrow -\infty} G_0(u) = 0$ while $\lim_{u \rightarrow +\infty} G_0(u) = 1$.

To derive (B.10), note that

$$\begin{aligned} |B_n| &= \left| \mathbb{E} w(\nu_0 u) \mathbb{I}_{u - \mathbf{x}^T \hat{\boldsymbol{\theta}} \leq \hat{\sigma} s} - \mathbb{E} w(\nu_0 u) \mathbb{I}_{u \leq \sigma_0 s} \right| \\ &\leq \mathbb{E} \left| \mathbb{I}_{u \leq \mathbf{x}^T \hat{\boldsymbol{\theta}} + \hat{\sigma} s} - \mathbb{I}_{u \leq \sigma_0 s} \right|. \end{aligned}$$

If $\mathbf{x}^T \hat{\boldsymbol{\theta}} + \hat{\sigma} s \leq \sigma_0 s$, then $\mathbb{I}_{u \leq \mathbf{x}^T \hat{\boldsymbol{\theta}} + \hat{\sigma} s} = 1$ implies that $\mathbb{I}_{u \leq \sigma_0 s} = 1$, so that $\Delta(u) = \mathbb{I}_{u \leq \mathbf{x}^T \hat{\boldsymbol{\theta}} + \hat{\sigma} s} - \mathbb{I}_{u \leq \sigma_0 s} = 0$. Similarly, if $\mathbb{I}_{u \leq \sigma_0 s} = 0$, then $\mathbb{I}_{u \leq \mathbf{x}^T \hat{\boldsymbol{\theta}} + \hat{\sigma} s} = 0$ and $\Delta(u) = 0$. Therefore, when $\mathbf{x}^T \hat{\boldsymbol{\theta}} + \hat{\sigma} s \leq \sigma_0 s$, $\Delta(u) = 1$ if and only if $\mathbf{x}^T \hat{\boldsymbol{\theta}} + \hat{\sigma} s < u \leq \sigma_0 s$.

On the other hand, if $\mathbf{x}^T \hat{\boldsymbol{\theta}} + \hat{\sigma} s \geq \sigma_0 s$, then $\Delta(u) = 1$ if and only if $\sigma_0 s < u \leq \mathbf{x}^T \hat{\boldsymbol{\theta}} + \hat{\sigma} s$.

Note that the fact that $\hat{\boldsymbol{\theta}} \xrightarrow{a.s.} 0$ and $\hat{\sigma} \xrightarrow{a.s.} \sigma_0$ entails that $\mathbf{x}^T \hat{\boldsymbol{\theta}} + \hat{\sigma} s \xrightarrow{a.s.} \sigma_0 s$, for each \mathbf{x} . Let $\mathcal{C} = \{\mathbf{x} : \mathbf{x}^T \hat{\boldsymbol{\theta}} + \hat{\sigma} s \leq \sigma_0 s\}$ and $\bar{\mathcal{C}}$ its complement, then

$$\begin{aligned} |B_n| &\leq \mathbb{E} \mathbb{I}_{\mathcal{C}} \mathbb{I}_{\mathbf{x}^T \hat{\boldsymbol{\theta}} + \hat{\sigma} s < u \leq \sigma_0 s} + \mathbb{E} \mathbb{I}_{\bar{\mathcal{C}}} \mathbb{I}_{\sigma_0 s < u \leq \mathbf{x}^T \hat{\boldsymbol{\theta}} + \hat{\sigma} s} \\ &\leq \mathbb{E} \mathbb{I}_{\mathcal{C}} \left\{ G_0(s) - G_0\left(\frac{\mathbf{x}^T \hat{\boldsymbol{\theta}} + \hat{\sigma} s}{\sigma_0}\right) \right\} + \mathbb{E} \mathbb{I}_{\bar{\mathcal{C}}} \left\{ G_0\left(\frac{\mathbf{x}^T \hat{\boldsymbol{\theta}} + \hat{\sigma} s}{\sigma_0}\right) - G_0(s) \right\} \\ &\leq \mathbb{E} \left| G_0\left(\frac{\mathbf{x}^T \hat{\boldsymbol{\theta}} + \hat{\sigma} s}{\sigma_0}\right) - G_0(s) \right| \end{aligned}$$

and (B.10) follows immediately from the continuity of G_0 and **C3**, concluding the proof of (B.8).

Similar arguments allow to show that

$$\frac{1}{n} \sum_{i=1}^n w_i \xrightarrow{a.s.} h_{\infty}(t_0) = \begin{cases} \mathbb{E}_{G_0} w \left(\frac{\epsilon_1}{t_0} \right) & \text{if } t_0 < \infty \\ 1 & \text{if } t_0 = \infty \end{cases} \quad (\text{B.11})$$

and the desired result follows now easily combining (B.8) and (B.11). ■

B.2 Non-linear Model

In this section, we assume that we have a random sample $(y_1, \mathbf{x}_1), \dots, (y_n, \mathbf{x}_n)$, where \mathbf{x}_i is a vector of p explanatory variables and y_i is a response variable that satisfy

$$y_i = f(\mathbf{x}_i, \boldsymbol{\beta}_0) + u_i = f(\mathbf{x}_i, \boldsymbol{\beta}_0) + \sigma_0 \epsilon_i, i = 1 \dots n,$$

with $\boldsymbol{\beta}_0 \in \mathbb{R}^q$ and the errors ϵ_i are i.i.d. and independent of \mathbf{x}_i with unknown distribution $G_0(\cdot)$ and σ_0 is the scale parameter. As above, the residuals are defined using robust strongly consistent estimators of $\boldsymbol{\beta}_0$ and σ_0 , let us say $\hat{\boldsymbol{\beta}}$ and $\hat{\sigma}$ as

$$r_i = \frac{y_i - f(\mathbf{x}_i, \hat{\boldsymbol{\beta}})}{\hat{\sigma}} = \frac{u_i - [f(\mathbf{x}_i, \hat{\boldsymbol{\beta}}) - f(\mathbf{x}_i, \boldsymbol{\beta}_0)]}{\hat{\sigma}}.$$

We compute the adaptive weighted empirical distribution at point t as in (6) with

$$w_i = w \left(\frac{r_i}{t_n} \right),$$

where as in Section B.1, the adaptive cut-off values are defined through (7).

The following additional assumptions are required to provide a general framework to deal with non-linear models.

C4 The class of functions

$$\mathcal{F} = \{f(\mathbf{x}, \boldsymbol{\beta}), \|\boldsymbol{\beta} - \boldsymbol{\beta}_0\| \leq 1\}$$

with envelope $F \in L^1(P_{\mathbf{x}})$ is such that $N_{[]}(\epsilon, \mathcal{F}, L_1(P_{\mathbf{x}})) < \infty$, where $P_{\mathbf{x}}$ is the probability measure of \mathbf{x} .

C5 G_0 has a bounded density g_0 .

C6 $f(\mathbf{x}, \boldsymbol{\beta})$ is a continuous function of $\boldsymbol{\beta}$ for each \mathbf{x} and $F(\mathbf{x}) = \sup_{\|\boldsymbol{\beta} - \boldsymbol{\beta}_0\| \leq 1} f(\mathbf{x}, \boldsymbol{\beta}) \in L^1(P_{\mathbf{x}})$.

It is worth noticing that Lemma 3.10 in van der Geer (2000) entails that **C4** holds if **C6** holds.

Lemma 4 below is an intermediate result needed to derive Lemma 5 which is the non-linear counterpart of Lemma 2.

Lemma 4. *Assume that **C2**, **C4** and **C5** hold. Denote $\mathcal{V}_0 = \{\boldsymbol{\beta} : \|\boldsymbol{\beta} - \boldsymbol{\beta}_0\| \leq 1\}$ and $\mathcal{I}_0 = [\sigma_0/2, 2\sigma_0]$ and for any fixed $t \geq 0$ consider the family of functions*

$$\mathcal{H} = \{h_{\boldsymbol{\beta}, \sigma}(y, \mathbf{x}) = \mathbb{I}_{|y - f(\mathbf{x}, \boldsymbol{\beta})| \leq \sigma t} \text{ for } (\boldsymbol{\beta}, \sigma) \in \mathcal{V}_0 \times \mathcal{I}_0\}.$$

Then, $\sup_{h \in \mathcal{H}} |P_n h - P h| \xrightarrow{a.s.} 0$.

PROOF. First, note that

$$h_{\boldsymbol{\beta}, \sigma}(y, \mathbf{x}) = \mathbb{I}_{|y - f(\mathbf{x}, \boldsymbol{\beta})| \leq \sigma t} = h_{\boldsymbol{\beta}, \sigma}^{(1)}(y, \mathbf{x}) h_{\boldsymbol{\beta}, \sigma}^{(2)}(y, \mathbf{x}),$$

where

$$\begin{aligned} h_{\beta, \sigma}^{(1)}(y, \mathbf{x}) &= \mathbb{I}_{y - f(\mathbf{x}, \beta) - \sigma t \leq 0} \\ h_{\beta, \sigma}^{(2)}(y, \mathbf{x}) &= \mathbb{I}_{0 \leq y - f(\mathbf{x}, \beta) + \sigma t} . \end{aligned}$$

Denote as $\mathcal{H}^{(j)} = \{h_{\beta, \sigma}^{(j)}(y, \mathbf{x}), (\beta, \sigma) \in \mathcal{V}_0 \times \mathcal{I}_0\}$. Taking into account that $\mathcal{H} \subset \mathcal{H}^{(1)} \cdot \mathcal{H}^{(2)}$ and that the functions $h_{\beta, \sigma}^{(j)}$ are non-negative and bounded by 1, to show that

$$\sup_{h \in \mathcal{H}} |P_n h - P h| \xrightarrow{a.s.} 0 ,$$

it will be enough to show that $N_{[]}(\epsilon, \mathcal{H}^{(j)}, L_1(P)) < \infty$, for $j = 1, 2$, where P is the probability measure of (y, \mathbf{x}) . We will derive the result for $\mathcal{H}^{(1)}$, the proof for $\mathcal{H}^{(2)}$ been analogous.

Let $\epsilon > 0$ and denote $\delta = \sigma_0 \epsilon / (2 \|g_0\|_\infty)$. Then, the fact that \mathcal{I}_0 is compact entails that there exist $k \leq 2t\sigma_0/\delta$ $\sigma_0/2 = \sigma_1 \leq \dots \leq \sigma_k = 2\sigma_0$ such that $\sigma_j - \sigma_{j-1} \leq \delta/t$.

Denote $M = N_{[]}(\delta, \mathcal{F}, L_1(P_{\mathbf{x}}))$, then there exists $\{(f_{j,L}, f_{j,U})\}_{1 \leq j \leq M}$ such that, for any $f \in \mathcal{F}$ there exists j such that $f_{j,L} \leq f \leq f_{j,U}$ and $\mathbb{E}f_{j,U} - f_{j,L} \leq \delta$.

Fix $\beta \in \mathcal{V}_0$ and $\sigma \in \mathcal{I}_0$ and let $1 \leq j \leq M$ and $1 \leq \ell \leq k-1$, be such that $\sigma \in [\sigma_\ell, \sigma_{\ell+1}]$ and $f_{j,L}(\mathbf{x}) \leq f(\mathbf{x}) \leq f_{j,U}(\mathbf{x})$, for all \mathbf{x} . Then, using that $t \geq 0$ we obtain that

$$g_{\ell,j,L}(y, \mathbf{x}) = y - f_{j,U}(\mathbf{x}) - \sigma_{\ell+1} t \leq y - f(\mathbf{x}, \beta) - \sigma t \leq y - f_{j,L}(\mathbf{x}) - \sigma_\ell t = g_{\ell,j,U}(y, \mathbf{x}) ,$$

so that

$$\mathbb{I}_{g_{\ell,j,U}(y, \mathbf{x}) \leq 0} \leq h_{\beta, \sigma}^{(1)}(y, \mathbf{x}) \leq \mathbb{I}_{g_{\ell,j,L}(y, \mathbf{x}) \leq 0} .$$

Denote $h_{\ell,j,L} = \mathbb{I}_{g_{\ell,j,U}(y, \mathbf{x}) \leq 0}$ and $h_{\ell,j,U} = \mathbb{I}_{g_{\ell,j,L}(y, \mathbf{x}) \leq 0}$. We will show that $\mathbb{E}|h_{\ell,j,U} - h_{\ell,j,L}| < \epsilon$, that is, $\{(h_{\ell,j,L}, h_{\ell,j,U})\}_{1 \leq \ell \leq M, 1 \leq j \leq k}$ is an ϵ -bracket for $\mathcal{H}^{(1)}$, so $N_{[]}(\epsilon, \mathcal{H}^{(1)}, L_1(P)) \leq kM < \infty$. Using that $h_{\ell,j,L} \leq h_{\ell,j,U}$, $g_{\ell,j,L}(y, \mathbf{x}) \leq g_{\ell,j,U}(y, \mathbf{x})$ and that

$$g_{\ell,j,L}(y, \mathbf{x}) = u + f(\mathbf{x}, \beta_0) - f_{j,U}(\mathbf{x}) - \sigma_{\ell+1} t \quad g_{\ell,j,U}(y, \mathbf{x}) = u + f(\mathbf{x}, \beta_0) - f_{j,L}(\mathbf{x}) - \sigma_\ell t$$

we get that

$$\begin{aligned}
\mathbb{E}|h_{\ell,j,U} - h_{\ell,j,L}| &= \mathbb{E}\mathbb{I}_{g_{\ell,j,L}(y,\mathbf{x}) \leq 0} - \mathbb{I}_{g_{\ell,j,U}(y,\mathbf{x}) \leq 0} = \mathbb{P}(g_{\ell,j,L}(y,\mathbf{x}) \leq 0) - \mathbb{P}(g_{\ell,j,U}(y,\mathbf{x}) \leq 0) \\
&= \mathbb{P}(u \leq f_{j,U}(\mathbf{x}) + \sigma_{\ell+1} t - f(\mathbf{x}, \beta_0)) - \mathbb{P}(u \leq f_{j,L}(\mathbf{x}) + \sigma_{\ell} t - f(\mathbf{x}, \beta_0)) \\
&= \mathbb{E} \left\{ G_0 \left(\frac{f_{j,U}(\mathbf{x}) + \sigma_{\ell+1} t - f(\mathbf{x}, \beta_0)}{\sigma_0} \right) - G_0 \left(\frac{f_{j,L}(\mathbf{x}) + \sigma_{\ell} t - f(\mathbf{x}, \beta_0)}{\sigma_0} \right) \right\}
\end{aligned}$$

Thus, using that G_0 has a bounded density g_0 , we obtain that

$$\begin{aligned}
\mathbb{E}|h_{\ell,j,U} - h_{\ell,j,L}| &\leq \|g_0\|_{\infty} \mathbb{E} \left\{ \left| \frac{f_{j,U}(\mathbf{x}) + \sigma_{\ell+1} t - f(\mathbf{x}, \beta_0)}{\sigma_0} - \frac{f_{j,L}(\mathbf{x}) + \sigma_{\ell} t - f(\mathbf{x}, \beta_0)}{\sigma_0} \right| \right\} \\
&\leq \frac{\|g_0\|_{\infty}}{\sigma_0} \{(\sigma_{\ell+1} - \sigma_{\ell}) t + \mathbb{E}|f_{j,U}(\mathbf{x}) - f_{j,L}(\mathbf{x})|\} \leq 2\delta \frac{\|g_0\|_{\infty}}{\sigma_0} = \epsilon,
\end{aligned}$$

concluding the proof. ■

Lemma 5. *Assume that **C2**, **C3**, **C5** and **C6** hold. Then, we have that*

a) $\|G_n^+ - G_0^+\|_{\infty} \xrightarrow{a.s.} 0$, where

$$G_n^+(t) = \frac{1}{n} \sum_{i=1}^n I(|r_i| \leq t) \quad r_i = \frac{y_i - f(\mathbf{x}_i, \hat{\beta})}{\hat{\sigma}}$$

and $G_0^+(t)$ is the distribution of the absolute errors when $\epsilon_i \sim G_0$

b) $d_n \xrightarrow{a.s.} d_0$.

c) $\bar{t}_n \xrightarrow{a.s.} \bar{t}_0$.

PROOF. a) Using Lemma 1, it will be enough to show that for each fixed t

$$G_n^+(t) - G_0^+(t) \xrightarrow{a.s.} 0. \tag{B.12}$$

Denote $\mathcal{V}_0 = \{\beta : \|\beta - \beta_0\| \leq 1\}$ and $\mathcal{I}_0 = [\sigma_0/2, 2\sigma_0]$. Let us consider the family of functions

$$\mathcal{H} = \{h_{\beta, \sigma}(y, \mathbf{x}) = \mathbb{I}_{|y - f(\mathbf{x}, \beta)| \leq \sigma t} \text{ for } (\beta, \sigma) \in \mathcal{V}_0 \times \mathcal{I}_0\}.$$

Using that **C6** implies **C4**, Lemma 4 entails that

$$\sup_{h \in \mathcal{H}} |P_n h - P h| \xrightarrow{a.s.} 0. \quad (\text{B.13})$$

On the other hand, G_n^+ can be written as

$$G_n^+(t) = P_n h_{\hat{\beta}, \hat{\sigma}}(y_i, \mathbf{x}_i).$$

Hence, if we denote as $M(\beta, \sigma) = P h_{\beta, \sigma}$, using (B.13) and the fact that **C3** entails that with probability 1, for n large enough, $(\hat{\beta}, \hat{\sigma}) \in \mathcal{V}_0 \times \mathcal{I}_0$, we conclude that

$$|G_n^+(t) - M(\hat{\theta}, \hat{\sigma})| \xrightarrow{a.s.} 0.$$

It remains to show that

$$M(\hat{\theta}, \hat{\sigma}) - G_0^+(t) \xrightarrow{a.s.} 0.$$

Note that

$$M(\beta, \sigma) = P h_{\beta, \sigma} = \mathbb{P}(|y - f(\mathbf{x}, \beta)| \leq \sigma t),$$

hence

$$M(\beta_0, \sigma_0) = \mathbb{P}(|u| \leq \sigma_0 t) = G_0^+(t).$$

Therefore, we have to show that

$$M(\hat{\theta}, \hat{\sigma} t) \xrightarrow{a.s.} M(\beta_0, \sigma_0).$$

First observe that

$$\begin{aligned} M(\beta, \sigma) &= \mathbb{P}(-\sigma t + f(\mathbf{x}, \beta) - f(\mathbf{x}, \beta_0) \leq u \leq \sigma t + f(\mathbf{x}, \beta) - f(\mathbf{x}, \beta_0)) \\ &= \mathbb{E} \{G_0(\sigma t + f(\mathbf{x}, \beta) - f(\mathbf{x}, \beta_0)) - G_0(-\sigma t + f(\mathbf{x}, \beta) - f(\mathbf{x}, \beta_0))\} \end{aligned}$$

The continuity of G_0 and $f(\mathbf{x}, \beta)$ and the Dominated Convergence Theorem entail that $M(\beta, \sigma)$ is a continuous function of its arguments, which together with **C3**, entails that $M(\hat{\theta}, \hat{\sigma}) - M(\beta_0, \sigma_0) \xrightarrow{a.s.} 0$, for each fixed t , concluding the proof of a).

b) and c) follow as in Lemma Lemma 2. ■

As in Section B.1, denote $\widehat{\nu}_n = 1/(t_n \widehat{\sigma}_n)$, $\nu_0 = 1/(t_0 \sigma_0)$, where we understand that if $t_0 = \infty$, $\nu_0 = 0$. Furthermore, let \mathcal{J}_0 be a compact interval with non-empty interior, such that $\nu_0 \in \mathcal{J}_0$.

Lemma 6 is the non-linear counterpart of Lemma 3. Note that a bounded density is needed when a general non-linear model is considered, as well as a continuous weight function.

Lemma 6. *Under **C1**, **C2**, **C5** and **C6**, we have that $\sup_{g \in \mathcal{G}} |P_n g - P g| \xrightarrow{a.s.} 0$, where*

$$\mathcal{G} = \{g_{\beta, \sigma, \nu}(y, \mathbf{x}) = w(\nu(y - f(\mathbf{x}, \beta))) \mathbb{I}_{y - f(\mathbf{x}, \beta) \leq \sigma t} \text{ for } (\beta, \sigma, \nu) \in \mathcal{V}_0 \times \mathcal{I}_0 \times \mathcal{J}_0\}.$$

PROOF. Note that $\mathcal{G} \subset \mathcal{G}_1 \cdot \mathcal{G}_2$ where

$$\begin{aligned} \mathcal{G}_1 &= \{g_{\beta, \nu}(y, \mathbf{x}) = w(\nu(y - f(\mathbf{x}, \beta))) \text{ for } (\beta, \nu) \in \mathcal{V}_0 \times \mathcal{J}_0\} \\ \mathcal{G}_2 &= \{g_{\beta, \sigma}(y, \mathbf{x}) = \mathbb{I}_{y - f(\mathbf{x}, \beta) \leq \sigma t} \text{ for } (\beta, \sigma) \in \mathcal{V}_0 \times \mathcal{I}_0\}. \end{aligned}$$

The classes \mathcal{G} , \mathcal{G}_1 and \mathcal{G}_2 have envelope 1 and are classes of non-negative functions, hence we have easily that,

$$N_{[\cdot]}(2\epsilon, \mathcal{G}, L_1(P)) \leq N_{[\cdot]}(\epsilon, \mathcal{G}_1, L_1(P)) N_{[\cdot]}(\epsilon, \mathcal{G}_2, L_1(P)),$$

so that to show $\sup_{g \in \mathcal{G}} |P_n g - P g| \xrightarrow{a.s.} 0$, it will be enough to prove that, for $j = 1, 2$,

$$N_{[\cdot]}(\epsilon, \mathcal{G}_j, L_1(P)) < \infty. \tag{B.14}$$

Note that, when $j = 2$, (B.14) follows from the proof of Lemma 4. On the other hand, the continuity of w and **C6** entail that $w(\nu(y - f(\mathbf{x}, \beta)))$ is a continuous function of (ν, β) for each (y, \mathbf{x}) . Then, Lemma 3.10 in van der Geer (2000) entails that $N_{[\cdot]}(\epsilon, \mathcal{G}_1, L_1(P)) < \infty$, concluding the proof. ■

Proposition 2. *Under **C1** to **C3** and **C5** and **C6**, we have that*

a) if $t_0 < \infty$,

$$\sup_{s \in \mathbb{R}} \left| \widehat{G}_n(s) - \frac{h_0(t_0, s)}{h_\infty(t_0)} \right| \xrightarrow{a.s.} 0,$$

with $h_\infty(t_0)$ and $h_0(t_0, s)$ defined in (B.1) and (B.2), respectively.

b) if $t_0 = \infty$, $\|\widehat{G}_n - G_0\|_\infty \xrightarrow{a.s.} 0$.

PROOF. When $t_0 = \infty$, using that G_0 is a bounded, monotone and continuous function and that \widehat{G}_n is monotone, from Lemma 1, it will be enough to show that for each $s \in \mathbb{R}$, $\widehat{G}_n(s) \xrightarrow{a.s.} G(s)$. On the other hand, when $t_0 < \infty$, standard arguments allow to show that $F(s) = h_1(t_0, s)/h_\infty(t_0)$ is a bounded, monotone and continuous function of s and the uniform convergence also follows from the pointwise one.

Taking into account that $\widehat{\nu}_n \xrightarrow{a.s.} \nu_0$, we have that with probability 1, for n large enough $\widehat{\nu}_n \in \mathcal{J}_0$.

As in the proof of Proposition 1, we will begin by showing that

$$\frac{1}{n} \sum_{i=1}^n w_i I(r_i \leq s) \xrightarrow{a.s.} h_0(t_0, s) = \begin{cases} \mathbb{E}_{G_0} w \left(\frac{\epsilon_1}{t_0} \right) \mathbb{I}_{\epsilon_1 \leq s} & \text{if } t_0 < \infty, \\ \mathbb{E}_{G_0} \mathbb{I}_{\epsilon_1 \leq s} = G_0(s) & \text{if } t_0 = \infty. \end{cases} \quad (\text{B.15})$$

For that purpose and noting that $r_i = (y_i - f(\mathbf{x}, \widehat{\boldsymbol{\beta}}))/\widehat{\sigma}$, define the class of functions

$$\mathcal{G} = \{g_{\boldsymbol{\beta}, \sigma, \nu}(y, \mathbf{x}) = w(\nu(y - f(\mathbf{x}, \boldsymbol{\beta}))) \mathbb{I}_{y - f(\mathbf{x}, \boldsymbol{\beta}) \leq \sigma s} \text{ for } (\boldsymbol{\beta}, \sigma, \nu) \in \mathcal{V}_0 \times \mathcal{I}_0 \times \mathcal{J}_0\}.$$

Lemma 6 entails that

$$\sup_{g \in \mathcal{G}} |P_n g - P g| \xrightarrow{a.s.} 0,$$

then, using that

$$\frac{1}{n} \sum_{i=1}^n w_i I(r_i \leq s) = P_n g_{\widehat{\boldsymbol{\beta}}, \widehat{\sigma}, \widehat{\nu}_n},$$

we obtain that

$$\frac{1}{n} \sum_{i=1}^n w_i I(r_i \leq s) - P g_{\widehat{\boldsymbol{\beta}}, \widehat{\sigma}, \widehat{\nu}_n} \xrightarrow{a.s.} 0.$$

It remains to show that

$$Pg_{\hat{\beta}, \hat{\sigma}, \hat{\nu}_n} \xrightarrow{a.s.} Pg_{\beta_0, \sigma_0, \nu_0} = h_0(t_0, s).$$

which will follow if we derive that

$$A_n = Pg_{\hat{\beta}, \hat{\sigma}, \hat{\nu}_n} - \mathbb{E}w(\nu_0 u) \mathbb{I}_{y-f(\mathbf{x}, \hat{\beta}) \leq \hat{\sigma} s} \xrightarrow{a.s.} 0 \quad (\text{B.16})$$

$$B_n = \mathbb{E}w(\nu_0 u) \mathbb{I}_{y-f(\mathbf{x}, \hat{\beta}) \leq \hat{\sigma} s} - h_0(t_0, s) \xrightarrow{a.s.} 0. \quad (\text{B.17})$$

Noting that

$$\begin{aligned} |A_n| &= \left| \mathbb{E} \left\{ w \left(\nu_n \left[y - f(\mathbf{x}, \hat{\beta}) \right] \right) - w(\nu_0 u) \right\} \mathbb{I}_{y-f(\mathbf{x}, \hat{\beta}) \leq \hat{\sigma} s} \right| \\ &\leq \mathbb{E} \left| w \left(\nu_n \left[y - f(\mathbf{x}, \hat{\beta}) \right] \right) - w(\nu_0 u) \right|, \end{aligned}$$

using the Dominated Convergence Theorem, the continuity of w and the fact that $\hat{\nu}_n \xrightarrow{a.s.} \nu_0$ and $\hat{\theta} \xrightarrow{a.s.} 0$, we obtain that $A_n \xrightarrow{a.s.} 0$, concluding the proof of (B.16).

To derive (B.17), using that $0 \leq w(x) \leq 1$, we get that

$$\begin{aligned} |B_n| &= \left| \mathbb{E}w(\nu_0 u) \mathbb{I}_{y-f(\mathbf{x}, \hat{\beta}) \leq \hat{\sigma} s} - \mathbb{E}w(\nu_0 u) \mathbb{I}_{u \leq \sigma_0 s} \right| \\ &\leq \mathbb{E} \left| \mathbb{I}_{u \leq f(\mathbf{x}, \hat{\beta}) - f(\mathbf{x}, \beta_0) + \hat{\sigma} s} - \mathbb{I}_{u \leq \sigma_0 s} \right|. \end{aligned}$$

As in the proof of Proposition 1, we have that, if $f(\mathbf{x}, \hat{\beta}) - f(\mathbf{x}, \beta_0) + \hat{\sigma} s \leq \sigma_0 s$, then $\Delta(u) = \mathbb{I}_{u \leq \mathbf{x}^T \hat{\theta} + \hat{\sigma} s} - \mathbb{I}_{u \leq \sigma_0 s} = 1$ if and only if $f(\mathbf{x}, \hat{\beta}) - f(\mathbf{x}, \beta_0) + \hat{\sigma} s < u \leq \sigma_0 s$.

On the other hand, if $f(\mathbf{x}, \hat{\beta}) - f(\mathbf{x}, \beta_0) + \hat{\sigma} s \geq \sigma_0 s$, then $\Delta(u) = 1$ if and only if $\sigma_0 s < u \leq f(\mathbf{x}, \hat{\beta}) - f(\mathbf{x}, \beta_0) + \hat{\sigma} s$.

Note that the fact that $\hat{\beta} \xrightarrow{a.s.} 0$ and $\hat{\sigma} \xrightarrow{a.s.} \sigma_0$ together with the continuity of $f(\mathbf{x}, \beta)$ entails that $f(\mathbf{x}, \hat{\beta}) - f(\mathbf{x}, \beta_0) + \hat{\sigma} s \xrightarrow{a.s.} \sigma_0 s$, for each \mathbf{x} . Let $\mathcal{C} = \{\mathbf{x} : f(\mathbf{x}, \hat{\beta}) - f(\mathbf{x}, \beta_0) + \hat{\sigma} s \leq \sigma_0 s\}$ and $\bar{\mathcal{C}}$ its complement, then

$$\begin{aligned} |B_n| &\leq \mathbb{E} \mathbb{I}_{\mathcal{C}} \mathbb{I}_{f(\mathbf{x}, \hat{\beta}) - f(\mathbf{x}, \beta_0) + \hat{\sigma} s < u \leq \sigma_0 s} + \mathbb{E} \mathbb{I}_{\bar{\mathcal{C}}} \mathbb{I}_{\sigma_0 s < u \leq f(\mathbf{x}, \hat{\beta}) - f(\mathbf{x}, \beta_0) + \hat{\sigma} s} \\ &\leq \mathbb{E} \left| G_0 \left(\frac{f(\mathbf{x}, \hat{\beta}) - f(\mathbf{x}, \beta_0) + \hat{\sigma} s}{\sigma_0} \right) - G_0(s) \right| \end{aligned}$$

and (B.17) follows immediately from the continuity of G_0 and **C3**, concluding the proof of (B.15).

Similar arguments allow to show that

$$\frac{1}{n} \sum_{i=1}^n w_i \xrightarrow{a.s.} h_{\infty}(t_0) = \begin{cases} \mathbb{E}_{G_0} w \left(\frac{\epsilon_1}{t_0} \right) & \text{if } t_0 < \infty \\ 1 & \text{if } t_0 = \infty \end{cases} \quad (\text{B.18})$$

and the desired result follows now easily combining (B.15) and (B.18). ■

References

- Alonzo, T. A. and Pepe, M. S. (2002). Distribution-free ROC analysis using binary regression techniques. *Biostatistics*, **3**, 421-432.
- Bianco, A. M. and Spano, P. (2019). Robust inference for nonlinear regression models. *Test*, **28**, 369-398.
- Cai, T. (2004). Semiparametric ROC regression analysis with placement values. *Bio statistics*, **5**, 45-60.
- Inácio de Carvalho, V., Jara, A., Hanson, T. E. and de Carvalho, M. (2013). Bayesian non-parametric ROC regression modeling, *Bayesian Analysis*, **8**, 623-646.
- Faraggi, D. (2003). Adjusting receiver operating characteristic curves and related indices for covariates. *Journal of the Royal Statistical Society, Ser. D*, **52**, 1152-1174.
- Farcomeni, A. and Ventura, L. (2012). An overview of robust methods in medical research. *Statistical Methods in Medical Research*, **21**, 111-133.
- Gervini, D. and Yohai, V. J. (2002). A class of robust and fully efficient regression estimators. *Annals of Statistics*, **30**, 583-616.
- Goncalves, L., Subtil, A., Oliveira, M. R. and Bermudez, P. (2014) Roc Curve Estimation: An Overview. *REVSTAT-Statistical Journal*, **12**, 1-20.

- González-Manteiga, W., Pardo-Fernández, J. C., and Van Keilegom, I. (2011). ROC curves in non-parametric location-scale regression models. *Scandinavian Journal of Statistics*, **38**, 169-184.
- Greco, L. and Ventura, L. (2011). Robust inference for the stress-strength reliability. *Statistical Papers*, **52**, 773-788.
- Kosorok, M. (2008). *Introduction to Empirical Processes and Semiparametric Inference*. Springer-Verlag, New York.
- Krzanowski, W. J. and Hand, D. J. (2009). *ROC curves for continuous data*. Chapman and Hall/CRC, Boca Raton.
- Pardo-Fernández, J. C., Rodríguez-Alvarez, M. X. and Van Keilegom, I. (2014). A review on ROC curves in the presence of covariates. *REVSTAT Statistical Journal*, **12**, 21-41.
- Pepe, M. S. (1997). A regression modelling framework for receiver operating characteristic curves in medical diagnostic testing. *Biometrika*, **84**, 595-608.
- Pepe, M. S. (1998). Three approaches to regression analysis of receiver operating characteristic curves for continuous test results. *Biometrics*, **54**, 124-135.
- Pepe, M. S. (2003). *The Statistical Evaluation of Medical Tests for Classification and Prediction*, Oxford University Press, New York.
- Rodríguez-Alvarez, M. X., Roca-Pardiñas, J., and Cadarso-Suárez, C. (2011a). ROC curve and covariates: extending the induced methodology to the non-parametric framework. *Statistics and Computing*, **21**, 483-495.
- Rodríguez-Alvarez, M. X., Tahoces, P. C., Cadarso-Suárez, C., and Lado, M. J. (2011b). Comparative study of ROC regression techniques—applications for the computer-aided diagnostic system in breast cancer detection. *Computational Statistics and Data Analysis*, **55**, 888-902.
- Sun, Y. and Genton, M. G. (2011). Functional boxplots. *Journal of Computational and Graphical Statistics*, **20**, 316-334.

- Van de Geer, S. (2000). *Empirical Processes in M-Estimation*, Cambridge University Press, United States of America.
- van der Vaart, A. and Wellner, J. (1996). *Weak Convergence and Empirical Processes. With Applications to Statistics*. Springer-Verlag, New York.
- Walsh, S. J. (1997). Limitations to the robustness of binormal ROC curves: effects of model misspecification and location of decision thresholds on bias, precision, size and power, *Statistics in Medicine*, **16**, 669-679.
- Yohai, V. J. (1987). High Breakdown-Point and High Efficiency Robust Estimates for Regression. *Annals of Statistics*, **15**, 642-656.